Article

sp Carbon Chains Surrounded by sp Carbon Double Helices: Directed Syntheses of Wirelike Pt(C#C)Pt Moieties That Are Spanned by Two P(CH)P Linkages via Alkene Metathesis

Laura de Quadras, Eike B. Bauer, Wolfgang Mohr, James C. Bohling, Thomas B. Peters, Jos Miguel Martn-Alvarez, Frank Hampel, and John A. Gladysz

J. Am. Chem. Soc., **2007**, 129 (26), 8296-8309• DOI: 10.1021/ja071612n • Publication Date (Web): 13 June 2007

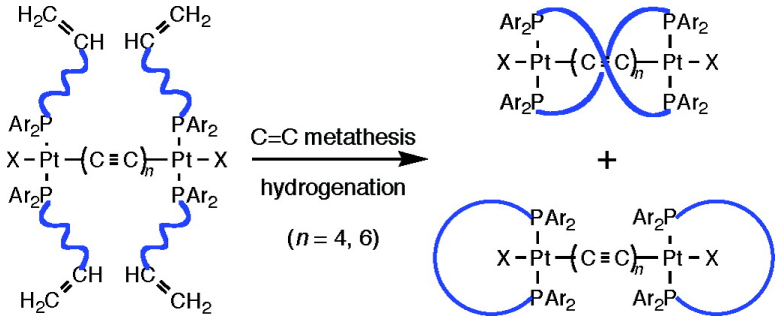

More About This Article

Additional resources and features associated with this article are available within the HTML version:

- Supporting Information
- Links to the 12 articles that cite this article, as of the time of this article download
- Access to high resolution figures
- Links to articles and content related to this article
- Copyright permission to reproduce figures and/or text from this article

View the Full Text HTML

J|A|C|S
ARTICLES
Published on Web 06/13/2007

sp Carbon Chains Surrounded by sp^3 Carbon Double Helices: Directed Syntheses of Wirelike $Pt(C{\equiv}C)_nPt$ Moieties That Are Spanned by Two $P(CH_2)_mP$ Linkages via Alkene Metathesis

Laura de Quadras,[†] Eike B. Bauer,[†] Wolfgang Mohr,[†] James C. Bohling,[‡] Thomas B. Peters,[‡] José Miguel Martín-Alvarez,[‡] Frank Hampel,[†] and John A. Gladysz*,[†]

Contribution from the Institut für Organische Chemie and Interdisciplinary Center for Molecular Materials, Friedrich-Alexander-Universität Erlangen-Nürnberg, Henkestraße 42, 91054 Erlangen, Germany, and Department of Chemistry, University of Utah, Salt Lake City, Utah 84112

Received March 13, 2007; E-mail: gladysz@chemie.uni-erlangen.de

Abstract: Reactions of *trans*-$(C_6F_5)(Ph_2P(CH_2)_{m'}CH{=}CH_2)_2PtCl$ (**1**; $m' =$ **a**, 6; **b**, 7; **c**, 8; **d**, 9; **e**, 10) and $H(C{\equiv}C)_2H$ ($HNEt_2$, cat. CuI) give *trans*-$(C_6F_5)(Ph_2P(CH_2)_{m'}CH{=}CH_2)_2Pt(C{\equiv}C)_2H$ (**3a**−**e**, 80−95%). Oxidative homocouplings of **3a**−**d** under Hay conditions (O_2, cat. CuCl/TMEDA, acetone) yield *trans*,*trans*-$(C_6F_5)(Ph_2P(CH_2)_{m'}CH{=}CH_2)_2Pt(C{\equiv}C)_4Pt(Ph_2P(CH_2)_{m'}CH{=}CH_2)_2(C_6F_5)$ (**4a**−**d**, 64−84%). Treatment of **3c**−**e** with excess $HC{\equiv}CSiEt_3$ under Hay conditions gives *trans*-$(C_6F_5)(Ph_2P(CH_2)_{m'}CH{=}CH_2)_2Pt(C{\equiv}C)_3SiEt_3$ (56−73%). Homocouplings (*n*-Bu_4N^+ F^-, Me_3SiCl, Hay conditions) afford *trans*,*trans*-$(C_6F_5)(Ph_2P(CH_2)_{m'}CH{=}CH_2)_2Pt(C{\equiv}C)_6Pt(Ph_2P(CH_2)_{m'}CH{=}CH_2)_2(C_6F_5)$ (**13c**−**e**, 59−64%). Reactions of **4a**−**d** and **13c**−**e** with Grubbs' catalyst, followed by hydrogenation, give mixtures of *trans*,*trans*-$(C_6F_5)(Ph_2P(CH_2)_mPPh_2)Pt(C{\equiv}C)_nPt(Ph_2P(CH_2)_mPPh_2)(C_6F_5)$ with termini-spanning diphosphines and *trans*,*trans*-$(C_6F_5)(Ph_2P(CH_2)_mPPh_2)Pt(C{\equiv}C)_nPt(Ph_2P(CH_2)_mPPh_2)(C_6F_5)$ with *trans*-spanning diphosphines ($m = 2m' + 2$; $n = 4, 6$). The latter ($n = 4$) are independently synthesized by similar metatheses/hydrogenations of **1a**−**d** to give *trans*-$(C_6F_5)(Ph_2P(CH_2)_mPPh_2)PtCl$ (49−59%), followed by analogous introductions of $(C{\equiv}C)_4$ chains (66−77%). Crystal structures of complexes with termini-spanning diphosphines show sp^3 chains with both double-helical ($m/n = 20/4$) and nonhelical ($m/n = 20/6$) conformations, and highly shielded sp chains. The sp^3 chains of complexes with *trans*-spanning diphosphines exhibit double half-clamshell conformations. The dynamic properties of both classes of molecules are analyzed in detail.

Introduction

Complexes in which wirelike sp carbon chains span two metals, $L_yMC_xML_y$, are of intense current interest.[1−3] They contain what can be regarded as the most fundamental type of unsaturated bridging ligand, which unlike nearly all others can never be twisted out of conjugation. Such species have a rich redox chemistry,[2,4,5] and the carbon chains can mediate a variety of charge- and electron-transfer processes.[6,7] However, some redox states are very labile and appear to decompose via bimolecular reactions involving the carbon chain.[4b] Hence, we have sought to sterically protect such species, hoping to expand the range of longer-lived redox states.[8]

In the preceding paper,[9] we described unprecedented coordination-driven self-assembly processes involving the pentafluorophenyl-substituted diplatinum polyynediyl complexes *trans*,*trans*-$(C_6F_5)(p\text{-}tol_3P)_2Pt(C{\equiv}C)_nPt(Pp\text{-}tol_3)_2(C_6F_5)$ ($n = 4$,

[†] Universität Erlangen-Nürnberg.
[‡] University of Utah.

(1) Bruce, M. I.; Low, P. J. *Adv. Organomet. Chem.* **2004**, *50*, 179.
(2) Paul, F.; Lapinte, C. In *Unusual Structures and Physical Properties in Organometallic Chemistry*; Gielen, M.; Willem, R.; Wrackmeyer, B., Eds.; Wiley: New York 2002; pp 220−291.
(3) Szafert, S.; Gladysz, J. A. *Chem. Rev.* **2003**, *103*, 4175; **2006**, *106*, PR1−PR33.
(4) (a) Brady, M.; Weng, W.; Zhou, Y.; Seyler, J. W.; Amoroso, A. J.; Arif, A. M.; Böhme, M.; Frenking, G.; Gladysz, J. A. *J. Am. Chem. Soc.* **1997**, *119*, 775. (b) Dembinski, R.; Bartik, T.; Bartik, B.; Jaeger, M.; Gladysz, J. A. *J. Am. Chem. Soc*. **2000**, *122*, 810. (c) Paul, F.; Meyer, W. E.; Toupet, L.; Jiao, H.; Gladysz, J. A.; Lapinte, C. *J. Am. Chem. Soc.* **2000**, *122*, 9405.
(5) Lead papers from other research groups: (a) Bruce, M. I.; Low, P. J.; Costuas, K.; Halet, J.-F.; Best, S. P.; Heath, G. A. *J. Am. Chem. Soc.* **2000**, *122*, 1949. (b) Coat, F.; Paul, F.; Lapinte, C.; Toupet, L.; Costuas, K.; Halet, J.-F. *J. Organomet. Chem.* **2003**, *683*, 368. (c) Venkatesan, K.; Fox, T.; Schmalle, H. W.; Berke, H. *Organometallics* **2005**, *24*, 2834.
(6) Long, N. J.; Williams, C. K. *Angew. Chem., Int. Ed.* **2003**, *42*, 2586; *Angew. Chem.* **2003**, *115*, 2690.
(7) Low, P. J. *Dalton Trans.* **2005**, 2821.
(8) (a) Meyer, W. E.; Amoroso, A. J.; Horn, C. R.; Jaeger, M.; Gladysz, J. A. *Organometallics* **2001**, *20*, 1115. (b) Horn, C. R.; Gladysz, J. A. *Eur. J. Inorg. Chem.* **2003**, *9*, 2211.
(9) Stahl, J.; Mohr, W.; de Quadras, L.; Peters, T. B.; Bohling, J. C.; Martín-Alvarez, J. M.; Owen, G. R.; Hampel, F.; Gladysz, J. A. *J. Am. Chem. Soc.* **2007**, *129*, 8282.

 10.1021/ja071612n CCC: $37.00

Scheme 1. Limiting Structures for Complexes Derived from $C_6F_5Pt(C{\equiv}C)_nPtC_6F_5$ Units and Diphosphines $Ar_2P(CH_2)_mPAr_2$ (**A**−**C**), and Synthetic Approach (**D, E**)

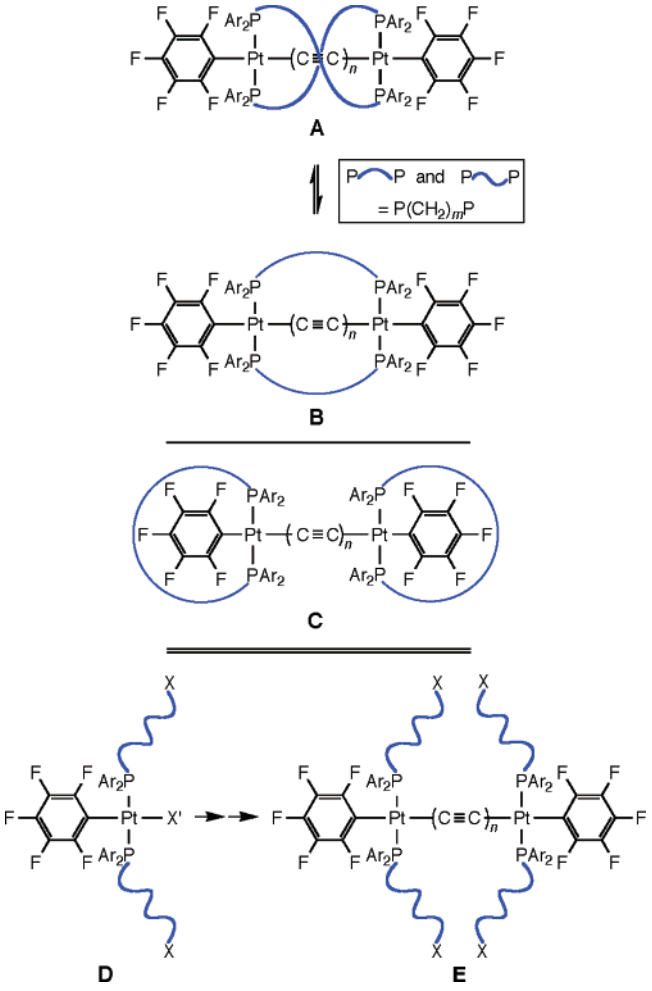

6) and bis(α,ω-diarylphosphino)alkanes $Ar_2P(CH_2)_mPAr_2$ (m = 10−12, 14, 18). These afford adducts with sterically shielded sp carbon chains, as illustrated by **A** and **B** in Scheme 1. When the polymethylene or sp³ chains are sufficiently long, chiral double-helical conformations **A** are possible. These are found crystallographically for n/m = 4/14 and 6/18 and as reported elsewhere for 3/14.[10] However, in solution they are in rapid equilibrium with achiral nonhelical conformations, such as **B**.

The complexes with n/m = 4/14 gave radical cations with stabilities significantly greater than analogues lacking sp³ carbon chains. However, with certain n/m combinations (4/16, 4/18, 4/32, 6/19, 6/20, 6/22, 6/24, 6/28, 8/28), only oligomeric products could be isolated. We wanted to expand the number of available complexes, so that the following types of questions could be addressed: (a) What is the maximum degree of helicity (sp³ chain twisting) possible for a given sp chain length? (b) Do more tightly twisted systems afford still longer lived radical cations and/or higher barriers for equilibration with **B**? (c) Are such barriers affected by the sp chain length?

Thus, an alternative synthetic strategy was investigated. This involved the binding of functionalized *mono*phosphines with $P(CH_2)_{m'}X$ linkages to platinum *prior* to attaching an sp carbon chain (**D**, Scheme 1). After generation of the polyynediyl bridge, the $P(CH_2)_{m'}X$ moieties would be joined by coupling reactions. This avoids phosphine substitution steps at all stages of the sequence and reduces the number of possibilities for oligomer formation. However, isomeric products **C** with *trans*-spanning diphosphine ligands might also be generated. Since the sp carbon chains in such complexes would also to some degree be sterically shielded, independent syntheses were incorporated into this study.

Following a democratic vote by the subset of authors who initiated this project a decade ago, a speculative coupling sequence involving alkene metathesis (**E** with X = CH═CH_2, Scheme 1) and C═C hydrogenation was selected. As detailed in the narrative below, this high-risk undertaking proved to be remarkably successful, significantly advancing the art of organometallic chemistry with respect to rational, directed syntheses of new metal-containing materials. Although the overall yields are moderate, the route is general and does not require "magic numbers" of sp and sp³ carbon atoms. A portion of this work has been communicated,[11] and additional details[12] and further extensions[13] are supplied elsewhere.

Results

1. $Pt(C{\equiv}C)_4Pt$ Complexes with Alkene-Containing Phosphine Ligands. Platinum chloride complexes of the formula *trans*-(Ar′)$(Ar_3P)_2PtCl$ are easily converted to platinum alkynyl species via Sonogashira-like reactions.[14] Accordingly, the chloride complexes *trans*-$(C_6F_5)(Ph_2P(CH_2)_{m'}CH{=}CH_2)_2PtCl$ (**1**; m' = **a**, 6; **b**, 7; **c**, 8; **d**, 9; **e**, 10) were prepared from the substitution-labile tetrahydrothiophene complex $[Pt(\mu\text{-}Cl)(C_6F_5)(tht)]_2$[15] and the corresponding alkene-containing diphenylphosphines $Ph_2P(CH_2)_{m'}CH{=}CH_2$ (**2**) as described earlier.[16,17]

As shown in Scheme 2, **1a**−**e** were combined with $H(C{\equiv}C)_2H$ under standard conditions ($HNEt_2$, cat. CuI). Workups gave the butadiynyl complexes **3a**−**e** as yellow or yellow-tan oils in 80−95% yields. Complexes **3a**−**e**, and all other new compounds below, were characterized by IR and NMR (^1H, ^{13}C, ^{31}P) spectroscopy and mass spectrometry, as summarized in the Experimental Section. In most cases, satisfactory microanalyses were also obtained. The IR and NMR properties of **3a**−**e** were similar to those of closely related platinum butadiynyl complexes.[14] The ^{31}P NMR spectra exhibited $^1J(^{31}P,^{195}Pt)$ couplings of approximately 2500 Hz, which is typical for *trans* platinum(II) bis(phosphine) complexes.[18]

We did not anticipate that the introduction of the butadiynyl ligand would be compromised by the vinyl groups in the phosphine ligands. However, we were not so sanguine with

(10) Owen, G. R.; Stahl, J.; Hampel, F.; Gladysz, J. A. *Organometallics* **2004**, *23*, 5889.

(11) (a) Stahl, J.; Bohling, J. C.; Bauer, E. B.; Peters, T. B.; Mohr, W.; Martín-Alvarez, J. M.; Hampel, F.; Gladysz, J. A. *Angew. Chem., Int. Ed.* **2002**, *41*, 1871; *Angew. Chem.* **2002**, *114*, 1951. (b) de Quadras, L.; Hampel, F.; Gladysz, J. A. *Dalton Trans.* **2006**, 2929.

(12) (a) Mohr, W. Doctoral Dissertation, Universität Erlangen-Nürnberg, 2002. (b) Bauer, E. B. Doctoral Dissertation, Universität Erlangen-Nürnberg, 2003. (c) de Quadras, L. Doctoral Dissertation, Universität Erlangen-Nürnberg, 2006.

(13) de Quadras, L.; Bauer, E. B.; Stahl, J.; Zhuravlev, F.; Hampel, F.; Gladysz, J. A. *New J. Chem.* **2007**. Manuscript submitted for publication.

(14) (a) Mohr, W.; Stahl, J.; Hampel, F.; Gladysz, J. A. *Chem.—Eur. J.* **2003**, *9*, 3324. (b) Zheng, Q.; Gladysz, J. A. *J. Am. Chem. Soc.* **2005**, *127*, 10508. (c) Zheng, Q.; Bohling, J. C.; Peters, T. B.; Frisch, A. C.; Hampel, F.; Gladysz, J. A. *Chem.—Eur. J.* **2006**, *12*, 6486.

(15) Usón, R.; Forniés, J.; Espinet, P.; Alfranca, G. *Synth. React. Inorg. Met.-Org. Chem.* **1980**, *10*, 579.

(16) Bauer, E. B.; Hampel, F.; Gladysz, J. A. *Organometallics* **2003**, *22*, 5567.

(17) (a) Lewanzik, N.; Oeser, T.; Blümel, J.; Gladysz, J. A. *J. Mol. Catal. A: Chem.* **2006**, *254*, 20. (b) de Quadras, L.; Stahl, J.; Zhuravlev, F.; Gladysz, J. A. *J. Organomet. Chem.* **2007**, *692*, 1859.

(18) Grim, S. O.; Keiter, R. L.; McFarlane, W. *Inorg. Chem.* **1967**, *6*, 1133.

Scheme 2. Syntheses of Diplatinum Octatetraynediyl Complexes with Alkene-Containing Phosphine Ligands[a]

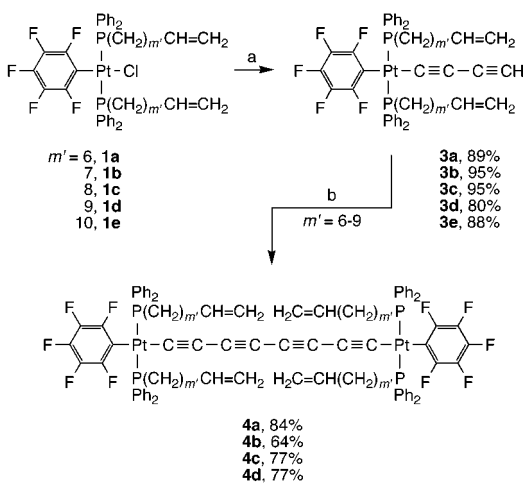

[a] Conditions: (a) $H(C{\equiv}C)_2H$, $HNEt_2$, cat. CuI; (b) O_2, acetone, cat. CuCl/TMEDA.

respect to subsequent oxidative homocouplings of **3**. Nonetheless, as shown in Scheme 2, when **3a**−**d** were reacted under Hay conditions (O_2, cat. CuCl/TMEDA, acetone), workups gave the octatetraynediyl or $Pt(C{\equiv}C)_4Pt$ complexes **4a**−**d** as yellow or tan oils in 64−84% yields. Again, the IR and NMR properties closely resembled those of related complexes.[14]

2. $Pt(C{\equiv}C)_4Pt$ Complexes with *trans*-Spanning Diphosphine Ligands. In order to better analyze alkene metathesis reactions of **4a**−**d**, authentic samples of the possible byproducts **C** (Scheme 1) were first prepared. As shown in Scheme 3, the chloride complexes **1a**−**d** were converted by a sequence involving alkene metathesis (Grubbs' first generation catalyst) and hydrogenation (10% Pd/C) to the 17-, 19-, 21-, and 23-membered macrocycles **5a**−**d** in 49−59% overall yields. The syntheses of **5a**,**c**,**d** have been reported previously.[16]

A reaction of **5a** and $H(C{\equiv}C)_2H$ analogous to those of **1a**−**e** in Scheme 2 afforded the butadiynyl complex **6a** in 86% yield. However, similar protocols were less effective with **5b**−**d**. Thus, **5b**−**d** were treated with the readily available bifunctional silyl/stannyl diyne $Me_3Sn(C{\equiv}C)_2SiMe_3$,[19] followed by CuI (0.2 equiv) and KPF_6 (1.1 equiv). Workups gave the trimethylsilylbutadiynyl complexes **7b**−**d** as white powders in 79−80% yields. Complex **6a** could be oxidized to the $Pt(C{\equiv}C)_4Pt$ complex **8a** in 84% yield under Hay conditions identical to those in Scheme 2. Complexes **7b**−**d** were first treated with wet *n*-Bu_4N^+ F^-, which effects protodesilylation to butadiynyl complexes. Then Me_3SiCl was added,[20] and the crude mixtures were similarly oxidized. Workups afforded **8b**−**d** as yellow powders in 84−90% yields.

The preceding complexes exhibited several distinctive properties. First, the mass spectra of **8a**−**d** showed molecular ions, but they were always less intense than monoplatinum fragment ions. In contrast, the mass spectra of the title complexes, which feature three bridging ligands linking the platinum atoms, always showed molecular ions that were much more intense than monoplatinum fragment ions.[9]

Scheme 3. Syntheses of Diplatinum Octatetraynediyl Complexes with *trans*-Spanning Diphosphine Ligands[a]

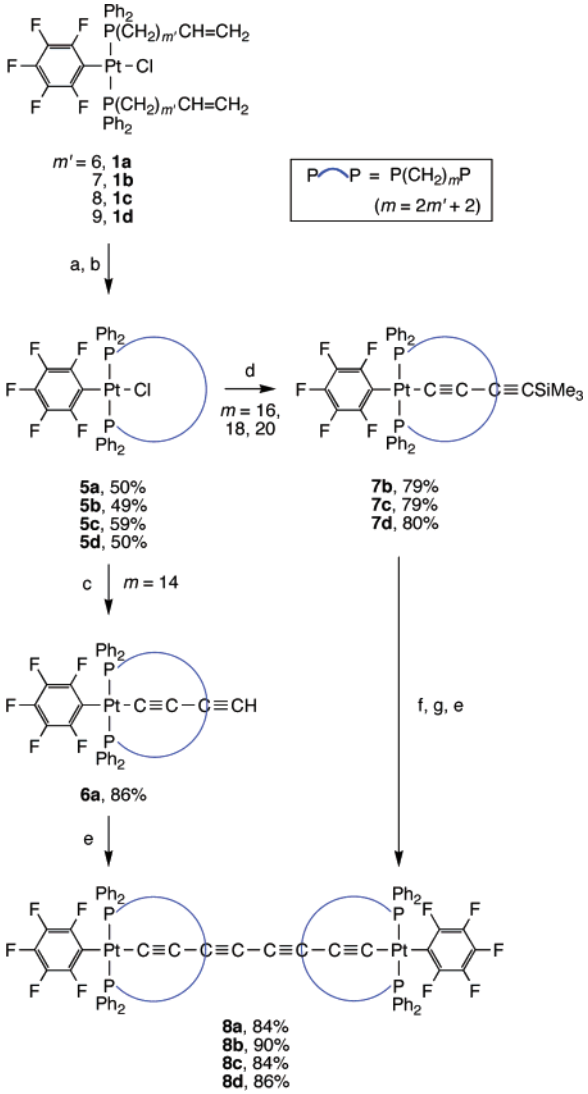

[a] Conditions: (a) 5−7 mol % Grubbs' Catalyst; (b) 10% Pd/C, 1 atm of H_2; (c) $H(C{\equiv}C)_2H$, $HNEt_2$, cat. CuI; (d) $Me_3Sn(C{\equiv}C)_2SiMe_3$, KPF_6, cat. CuI; (e) O_2, acetone, cat. CuCl/TMEDA; (f) wet *n*-Bu_4N^+ F^-; (g) Me_3SiCl.

Second, the PPh_2 groups and methylene protons in **5**−**8** are diastereotopic and can, in principle, give separate NMR signals. However, as analyzed in detail elsewhere,[16,21] net exchange occurs when *one* of the platinum ligands is small enough to pass through the macrocycle by rotation about the P−Pt−P axis. This is facile for the chloride ligand in **5a**[16,21] and by extension the higher homologues **5b**−**d**. With the 17- and 19-membered macrocycles **6a**, **7b**, and **8a**−**b**, two sets of PPh_2 ^{13}C NMR signals as well as PCH_2 and PCH_2CH_2 ^1H NMR signals are observed at room temperature (Figures s1−s3, Supporting Information). Hence, passage of the pentafluorophenyl *and* polyynyl ligands through the macrocycles is slow on the NMR time scale.[22]

In contrast, the 21- and 23-membered macrocycles **7c**,**d** and **8c**,**d** exhibit only a single set of NMR signals. Thus, passage

(19) (a) Bunz, U. H. F.; Enkelmann, V. *Organometallics* **1994**, *13*, 3823 (see footnote 14). (b) Zheng, Q.; Hampel, F.; Gladysz, J. A. *Organometallics* **2004**, *23*, 5896.

(20) This reagent, which is necessary for the success of the couplings,[14] is believed to serve as a F^- ion scavenger.

(21) Skopek, K.; Hershberger, M.; Gladysz, J. A. *Coord. Chem. Rev.* **2007**, in press (DOI: 10.1016/j.ccr.2006.12.015).

(22) There are additional subtleties associated with these processes, as diagrammed elsewhere.[12b,c] For example, for net exchange of diastereotopic groups in **8a**−**d**, both pentafluorophenyl ligands must pass through their respective macrocycles.

Table 1. Key Crystallographic Distances [Å] and Angles [deg]

complex	**7b** (molecule 1)	**7b** (molecule 2)	**8a**·EtOH[a]	**8c**·(C_6H_{12})[a]	**8d**[a]	**11d**	**14d**[a]
Pt · · · Pt(Si)	7.627	7.558	12.935	12.901	12.780	12.781(3)	18.0247(5)
sum of bond lengths, Pt1 to Pt2(Si)	7.633	7.633	12.952	12.922	12.891	12.899	18.056
Pt1−C1	2.007(4)	2.004(4)	1.985(5)	1.989(3)	1.976(3)	1.978(5)	1.984(6)
C1−C2	1.204(6)	1.214(6)	1.221(8)	1.217(5)	1.218(4)	1.222(7)	1.227(8)
C2−C3	1.373(6)	1.367(6)	1.368(8)	1.365(5)	1.367(5)	1.366(7)	1.370(9)
C3−C4	1.212(6)	1.218(6)	1.217(8)	1.211(5)	1.209(5)	1.193(7)	1.205(8)
C4−C5(Si)	1.834(5)	1.830(5)	1.370(2)	1.358(7)	1.351(7)	1.371(8)	1.347(9)
C5−C6	-	-	-	-	-	1.203(8)	1.214(9)
C6−C7(C6′)	-	-	-	-	-	1.358(7)	1.362(13)
C7−C8	-	-	-	-	-	1.216(7)	-
C8−Pt2	-	-	-	-	-	1.992(6)	-
Pt1−C1−C2	177.9(4)	179.1(4)	175.9(6)	177.5(3)	169.6(3)	174.4(5)	174.9(5)
C1−C2−C3	177.7(5)	173.9(5)	178.3(8)	175.7(4)	175.2(4)	176.4(6)	177.8(7)
C2−C3−C4	178.6(6)	176.5(5)	177.8(8)	177.9(4)	176.8(4)	176.3(7)	178.5(8)
C3−C4−C5(Si)	178.6(5)	169.3(4)	179.0(11)	177.7(6)	179.3(5)	176.0(7)	178.4(8)
C4−C5−C6	-	-	-	-	-	176.0(7)	178.8(9)
C5−C6−C7(C6′)	-	-	-	-	-	178.9(7)	179.1(12)
C6−C7−C8	-	-	-	-	-	179.5(7)	-
C7−C8−Pt2	-	-	-	-	-	175.0(5)	-
av Pt−C*sp*−C*sp*	177.9	179.1	175.9	177.5	169.6	174.7	174.9
av C*sp*−C*sp*−C*sp*	178.1	173.2	178.4	177.1	177.1	177.2	178.5
av sp/sp³ distance[b]	-	-	4.118	4.202	4.214	4.133[c]	3.999
av π stacking[d]	3.842	3.766	3.680	3.744	3.815	3.810	3.705
distance Pt to distal carbons[e]	7.345, 7.804	8.197, 8.728	7.191, 7.662	8.799, 9.594	10.561, 10.594	-	-
minus van der Waals radius of carbon (Å)[f,g]	6.104	7.028	5.962	7.894	8.861	-	-
P−Pt−P/Pt angle[h]	-	-	0	0	0	294.8	0
Pt+P+P+C_i+C1 angle[h]	-	-	0	0	0	297.5	0

[a] This molecule exhibits an inversion center. [b] Average distance from every CH_2 group to the Pt−Pt vector. [c] Helix pitch, 15.61; degree of helicity, 81.9%. [d] Distance between midpoints of the C_6F_5 and C_6H_5 rings. [e] The two carbon atoms in the middle of the methylene chain. [f] With respect to previous table entry. [g] The shortest platinum−carbon distance is used. [h] Angle between planes defined by these atoms on each endgroup.

of the pentafluorophenyl ligand through these larger rings is rapid on the NMR time scale (crystal structures below show that the polyynyl ligands are too long). In order to further characterize these processes, variable temperature spectra of representative complexes were recorded. As illustrated in the Supporting Information, the PC*HH*′ and PCHH′C*HH*′ ^{1}H NMR signals of **8b** did not decoalesce at 120 °C in toluene-d_8. Application of the coalescence formula ($\Delta\upsilon$ 103.9 Hz, PC*HH*′)[23] established a lower limit of 18.9 kcal/mol ($\Delta G^{\ddagger}$, 120 °C) for the exchange barrier. When ^{1}H and ^{13}C NMR spectra of **8c** were recorded at −115 °C in $CDFCl_2$, no decoalescence or significant line broadening was observed.

Complexes **8a**,**c**−**d** or solvates thereof could be crystallized. The crystal structures were solved as summarized in the Supporting Information. Key metrical parameters are given in Table 1.

As shown in Figure 1, the macrocycles exhibit double half-clamshell conformations of idealized C_{2h} symmetry that considerably shield the sp carbon chains. The crystal structure of the trimethylsilylbutadiynyl complex **7b** was also determined. As shown in Figure 2, two independent molecules were found in the unit cell. In one, the trimethylsilyl group was disordered; in the other, two sp³ carbon atoms were disordered. Only the major conformations are depicted. Other data for **7b** are incorporated into Table 1.

The distances from the platinum atoms to the *p*-fluorine atoms in **7b** and **8a**,**c**−**d** range from 6.21 to 6.25 Å. When the van der Waals radius of fluorine is added (1.47 Å),[24] the effective radius of the PtC_6F_5 moiety is obtained (7.68−7.72 Å). This can be compared to the distances from platinum to distal carbons of the macrocycle, i.e., the two in the middle of the methylene chain (Table 1). When the van der Waals radius of carbon (1.70 Å) is subtracted from the lower value, a "bridge height" is obtained. In the case of **8c** and **8d**, there is sufficient "clearance" for the PtC_6F_5 moiety to pass under the bridge (7.89 Å and 8.61 Å vs 7.68−7.72 Å). However, with **7b** and **8a** the values are too small (6.10−7.03 Å and 5.96 Å), in accord with the NMR properties. A similar analysis for the PtC≡CC≡C$SiMe_3$ moiety of **7b** gives a much greater radius (10.59 Å using a hydrogen atom of a methyl group).

3. Double-Helical Pt(C≡C)$_4$Pt Complexes. With the above compounds in hand, the stage was set for the title sequence in Scheme 4. On paper, alkene metatheses of **4a**−**d** are fraught with potential complications. In addition to undesired intermolecular condensations, the intermediate catalyst-bound alkylidene (RCH═M) might add to a C≡C bond, per the key step in enyne metathesis.[25] Nonetheless, the reaction of **4a** (ca. 0.001 M in CH_2Cl_2) and Grubbs' catalyst (7 mol %) smoothly gave a mixture of metathesis products in 96% yield after workup. The C/H microanalysis was in agreement with the isomeric complexes **9a**, with termini-spanning diphosphine ligands, and **10a**, with *trans*-spanning diphosphine ligands. The most intense peak in the mass spectrum was a monoplatinum ion, followed by

(23) Ōki, M. *Applications of Dynamic NMR Spectroscopy to Organic Chemistry*; VCH: 1985.

(24) Bondi, A. *J. Phys. Chem.* **1964**, *68*, 441.

(25) Diver, S. T.; Giessert, A. J. *Chem. Rev.* **2004**, *104*, 1317.

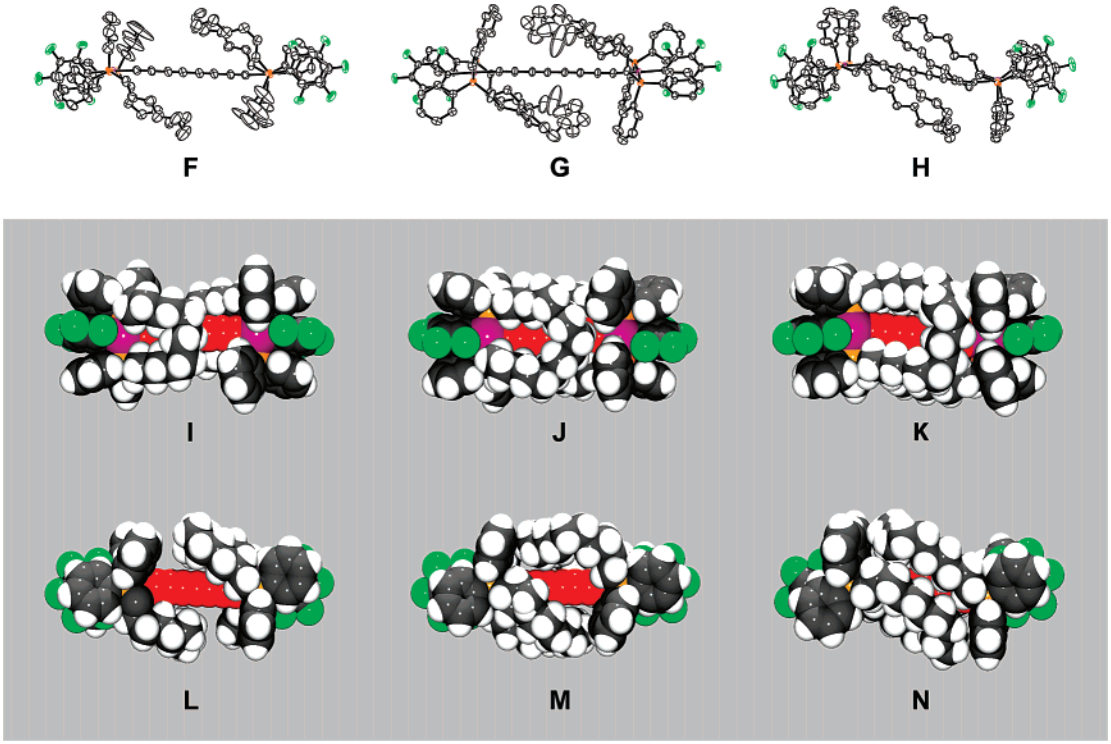

Figure 1. Thermal ellipsoid plots (50% probability level) of **8a**·EtOH (**F**), **8c**·(C_6H_{12}) (**G**; dominant conformation), and **8d** (**H**) with hydrogen and solvate molecules omitted, and views parallel (**I, J, K**) and perpendicular (**L, M, N**) to the C_6F_5 planes with atoms at van der Waals radii.

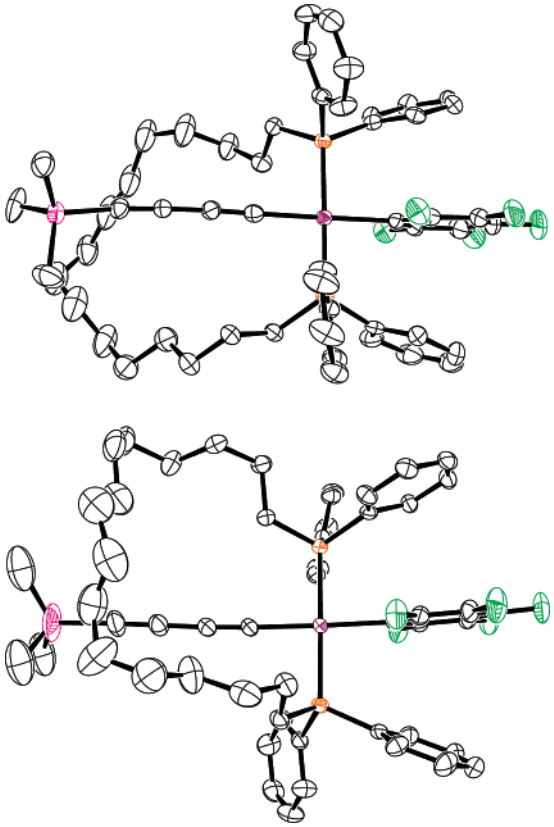

Figure 2. Thermal ellipsoid plots (50% probability level) of the dominant conformations of the two independent molecules in crystalline **7b** with hydrogen atoms omitted.

the molecular ion (60%). No triplatinum or tetraplatinum ions were detected.

The ^{1}H NMR spectrum showed no vinyl residues, indicating metathesis to be ≥98% complete. New CH═CH signals were apparent (δ 5.35−5.37). A ^{31}P NMR spectrum exhibited six peaks with a 12:30:24:22:7:6 area ratio. Although six *E*/*Z* isomers of **9a** and **10a** are possible, oligomers might also account for some signals. With four peaks, $^1J(^{31}P,^{195}Pt)$ couplings of ca. 2500 Hz were apparent, characteristic of *trans* platinum(II) bis(phosphine) complexes.[18]

To simplify analysis, we sought to reduce the C═C bonds of **9a**/**10a** without affecting the C≡C bonds. We were unaware of any precedent for such chemoselectivity with organic compounds. However, as shown in Scheme 4, palladium-catalyzed hydrogenation proved successful. In order to avoid over-reductions, and to work up incomplete reactions, low H_2 pressures and extended reaction periods (7−14 d) were employed. Alumina filtrations gave the crude product mixtures in 73−93% yields. These were expected to consist mainly of **11a** and **8a**, which were independently synthesized in the preceding paper[9] and Scheme 3, respectively.

The ^{1}H NMR spectra of the mixtures showed that all of the CH═CH linkages had been reduced. The mass spectra exhibited strong molecular ions. However, a ^{31}P NMR spectrum of a typical mixture showed five signals in a 40:35:16:5:4 ratio, corresponding to **11a**, **8a**, and three byproducts. Since the byproducts were not evident in the mass spectra, they were presumed to be oligomeric. Column chromatography of one sample afforded a **11a**/**8a** mixture in 33% yield. Preparative thin layer chromatography of another afforded **11a** as a yellow powder in 32% yield.

As summarized in Scheme 4, analogous sequences were conducted with **4b**−**d**, which feature longer sp^3 carbon segments. The crude metathesis products (96−97%) were not analyzed but rather directly hydrogenated. Chromatography gave the target molecules **11b**−**d**, with termini-spanning diphosphine ligands, in 15−48% yields. In the last two reactions, **8c**,**d**, with

Scheme 4. Syntheses of Diplatinum Octatetraynediyl Complexes with Termini-Spanning Diphosphine Ligands[a]

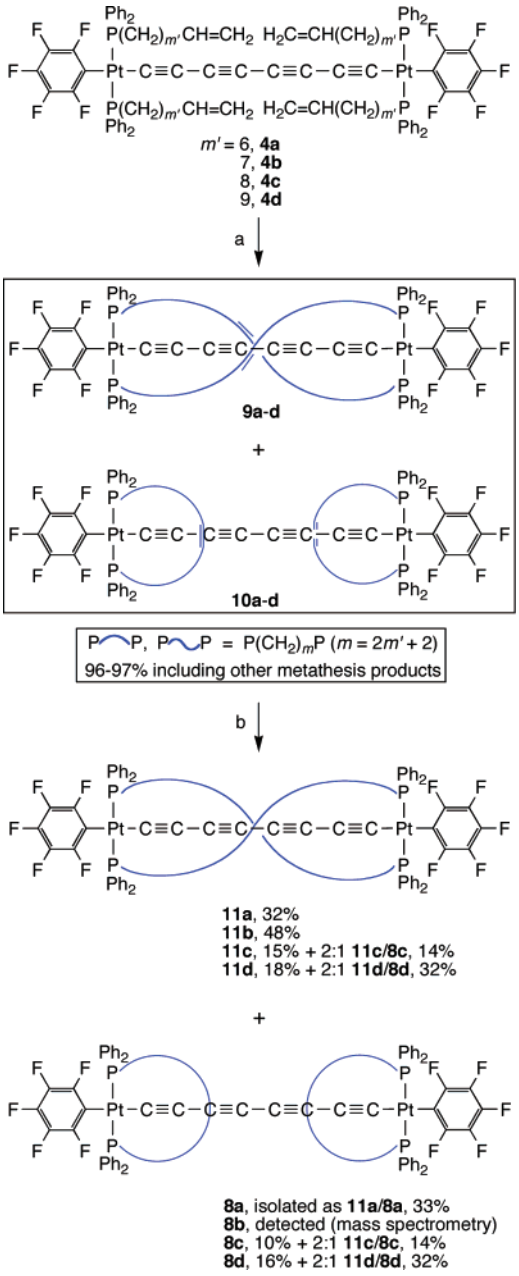

[a] Conditions: (a) 5−7 mol % Grubbs' catalyst (b) 10% Pd/C, 1 atm of H_2.

trans-spanning diphosphine ligands, were also isolated in 10% and 16% yields. Intermediate fractions afforded 2:1 **11c**/**8c** and **11d**/**8d** mixtures (14% and 32% yields). The formation of some **8b** could be verified by the characteristic mass spectral fragmentation pattern.

Importantly, **11b**−**d** could not be accessed by the route described in the preceding paper.[9] None of these complexes showed any tendency to oligomerize. Crystals of **11d**, in which the sp³ chains contain 20 carbon atoms, were obtained. The structure was determined analogously to those above. Key metrical parameters are summarized in Table 1. As shown in Figure 3 (top), a chiral double-helical conformation was found, with both enantiomers in the unit cell. As detailed in the Experimental Section, a nine-atom segment of one sp³ chain was disordered over multiple positions, and the best solution with all hydrogen atoms is depicted.

The angle defined by the P−Pt−P/P planes of **11d**, 294.8° (81.9% helicity), corresponds to more than three-quarters of a twist. This is significantly greater than that of the lower homologue **11a** in the preceding paper, which features sp³ chains containing 14 carbon atoms (196.5°−196.6° or 54.6% helicity).[9] As illustrated by the space-filling representations **P** and **Q** (Figure 3), the sp chain is nearly completely shielded.

The average distance of the sp³ carbon atoms from the platinum−platinum vector in **11d** approximates the radius of the double helix. This value, 4.13 Å, is greater than those of the four homologues with diphosphines of the formula $Ar_2P(CH_2)_{14}PAr_2$ in the preceding paper (3.76−3.90 Å),[9] indicative of a "looser" helix. Interestingly, **11d** is the first diplatinum polyynediyl species *trans*,*trans*-$(X)(R_3P)_2Pt(C{\equiv}C)_nPt(PR_3)_2(X)$ ($n \geq 3$; R = alkyl, Ar) among more than 16 examples[3,9,10,14,19b,26] to crystallize *without* nearly coplanar endgroups.

4. Pt(C≡C)$_6$Pt Complexes. Dodecahexaynediyl complexes with sp³ chains of greater than 18 carbon atoms could not be accessed by the route in the preceding paper.[9] Thus, as shown in Scheme 5, the butadiynyl complexes **3c**−**e** were treated with excess HC≡CSiEt$_3$ under Hay cross-coupling conditions. In accord with much precedent,[14] workups gave the triethylsilylhexatriynyl complexes **12c**−**e** as yellow oils in 56−73% yields. In all cases, minor amounts of the homocoupling products **4c**−**e** (9−19%) were also isolated.

Complexes **12c**−**e** were treated with wet *n*-Bu_4N^+ F^- to generate the corresponding hexatriynyl complexes, which are known for related systems to be quite labile. After addition of Me_3SiCl,[20] Hay homocoupling conditions afforded the Pt(C≡C)$_6$Pt complexes **13c**−**e** as yellow oils or solids in 59−64% yields. The properties of **12c**−**e** and **13c**−**e** were similar to those of related complexes with other phosphine ligands.[14]

Complexes **13c**−**e** were subjected to metathesis/hydrogenation sequences analogous to those in Scheme 4. In all cases, mixtures of products with termini-spanning diphosphine ligands (**14c**−**e**) and *trans*-spanning diphosphine ligands (**15c**−**e**) were obtained. Chromatography gave pure **14c** and **14d**, which feature sp³ chains with 18 and 20 carbon atoms, as yellow powders in 15−18% overall yields. The former complex was described in the preceding paper.[9] Analyses of other fractions by mass spectrometry showed the formation of **15c**,**d**, as inferred by fragmentation patterns analogous to those of **8a**−**d**. However, **14e** could not be separated from **15e** (combined overall yield 38%). Complexes **14c**−**e** showed no tendency to convert to insoluble oligomers.

Crystals of **14d** were obtained, and the structure was determined analogously to those above. Metrical parameters are summarized in Table 1. As shown in Figure 3 (bottom), a nonhelical conformation was found. This was a moderate surprise, as the lower homologue **14c** features both helical and nonhelical molecules in the unit cell,[9] and the two additional sp³ carbon atoms in each chain of **14d** should have facilitated the necessary twisting. Thus, for Pt(C≡C)$_6$Pt systems, sp³ chains

(26) (a) Wong, W.-Y.; Wong, C.-K.; Lu, G. L.; Cheah, K.-W.; Shi, J.-X.; Lin, Z. *J. Chem. Soc., Dalton Trans.* **2002**, 4587. (b) See also: Yam, V. W.-W.; Wong, K. M.-C.; Zhu, N. *Angew. Chem., Int. Ed.* **2003**, *42*, 1400; *Angew. Chem.* **2003**, *115*, 1438.

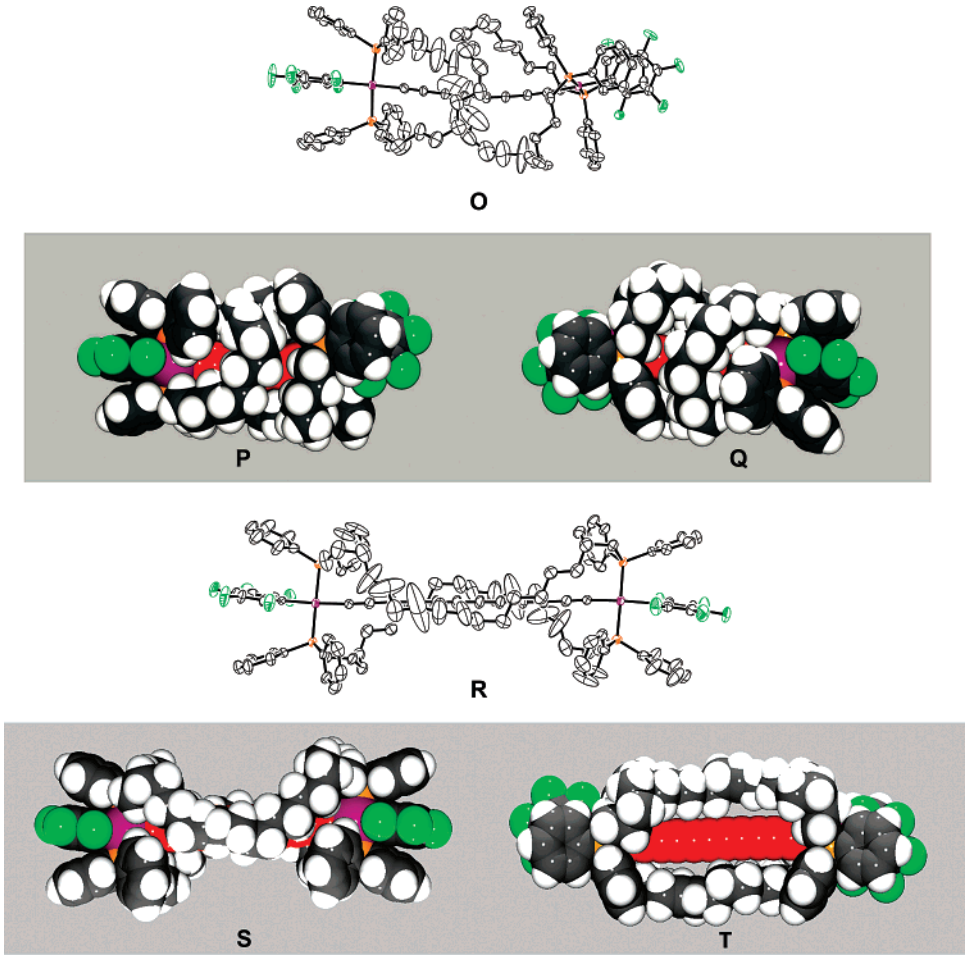

Figure 3. Thermal ellipsoid plots (50% probability level) of **11d** (**O**; dominant conformation) and **14d** (**R**) with hydrogen atoms omitted, and views parallel (**P, S**) and perpendicular (**Q, T**) to the C_6F_5 planes with atoms at van der Waals radii.

with 18−20 carbon atoms apparently constitute the transition regime between nonhelical and helical structures.

Starting from either of the phosphorus atoms of **14d** in the top portion of view **R** or **S** (Figure 3), the sp^3 chain initially descends. However, rather than connecting to an anti phosphorus atom in the bottom portion, the sp^3 chain turns parallel to the sp chain and eventually ascends to the opposite syn phosphorus atom in the top portion. The net result is a two-dimensional steric insulation, which leaves the sp chain distinctly exposed on two sides, as illustrated in **T**. The average distance of the sp^3 carbon atoms from the platinum−platinum vector (4.00 Å) is slightly greater than those in the helical and nonhelical forms of **14c** (3.91 and 3.98 Å).

5. Additional Experiments. In order to compare the redox properties of the above complexes to those in the preceding paper, cyclic voltammograms were recorded under identical conditions. Data are summarized in Table 2, and representative traces are given in the Supporting Information. Oxidations were observed, presumably to mixed valent platinum(II)/platinum(III) species. The reversibilities were fair to moderate, and the principal trends are analyzed below.

Another redox issue involves the chemoselectivities of the hydrogenations in Schemes 4 and 5. We wondered whether the $P(CH_2)_{m'}CH{=}CH(CH_2)_{m'}P$ segments might shield the sp carbon chain from the catalyst, favoring C=C hydrogenation. Hence, the unshielded octatetraynediyl complex *trans*,*trans*-$(C_6F_5)(p\text{-}tol_3P)_2Pt(C{\equiv}C)_4Pt(P\textit{p}\text{-}tol_3)_2(C_6F_5)$[14] was subjected to similar conditions. After 3 d, workup gave ca. 97% of the original sample mass. The ^{31}P NMR spectrum showed two peaks (90:10), with the major signal corresponding to educt. The ^1H NMR spectrum exhibited only trace signals in the methylene region (relative integral 2.1:36 vs the methyl groups).

The reaction was repeated under 30 atm of H_2. After 16 h, workup gave ca. 92% of the original sample mass. The ^{31}P NMR spectrum showed three peaks (81:16:3), with the major signal corresponding to the educt *trans*,*trans*-$(C_6F_5)(p\text{-}tol_3P)_2Pt(C{\equiv}C)_4Pt(P\textit{p}\text{-}tol_3)_2(C_6F_5)$. The ^1H NMR spectrum again exhibited trace signals in the methylene region (relative integral 2.6:36). Hence, we conclude that the C≡C linkages in the diplatinum octatetraynediyl complexes are intrinsically less reactive than disubstituted alkenes under the hydrogenation conditions utilized.

When **11** and **8** were heated in capillaries, there was no sign of decomposition below 150 °C or melting at much higher temperatures. TGA measurements showed no mass loss below 243 °C. DSC measurements with **11a**,[9] **11b**, and **8a** established particularly high stabilities (T_e = 244.0 (endotherm), 249.6 (exotherm), 210.1 (endotherm) °C). However, **11d**, **8c**, and **8d** exhibited exotherms at much lower temperatures (T_e = 113.2, 100.7, 154.7 °C), in some cases followed by endotherms. With **8b**, three endotherms were observed (T_e = 126.5, 182.9, 217.4 °C). These phenomena raise the possibility of solid state isomerizations or oligomerizations (exotherms) and/or phase transitions (endotherms). However, further investigations of

Scheme 5. Syntheses of Diplatinum Dodecahexaynediyl Complexes with Termini- or *trans*-Spanning Diphosphines[a]

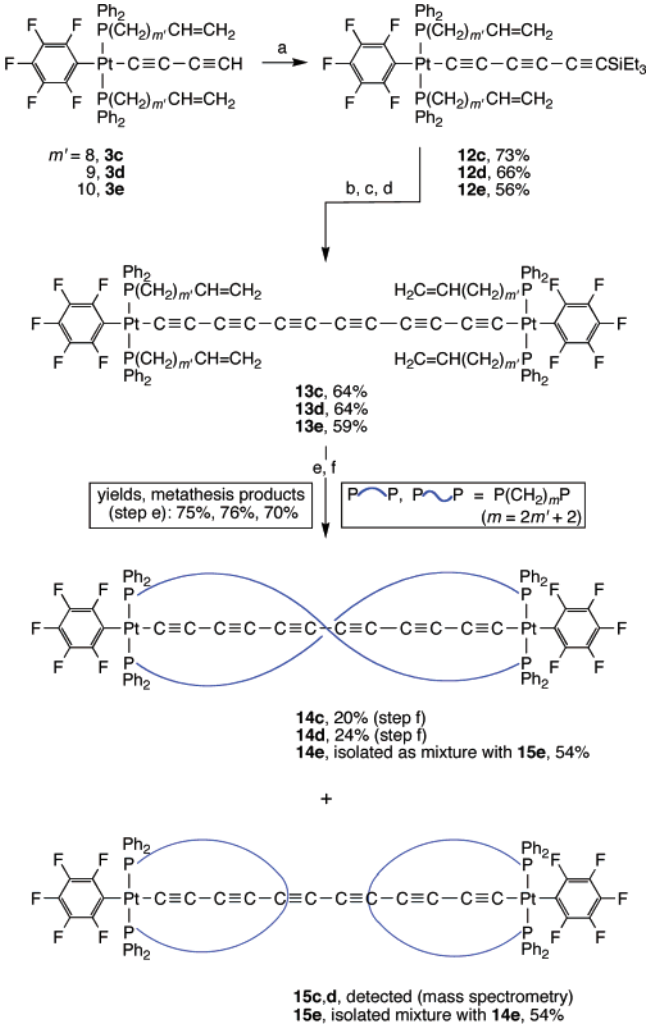

[a] Conditions: (a) HC≡CSiEt$_3$, O$_2$, acetone, cat. CuCl/TMEDA; (b) wet *n*-Bu$_4$N$^+$ F$^-$; (c) Me$_3$SiCl; (d) O$_2$, acetone, cat. CuCl/TMEDA; (e) 5−7 mol % Grubbs' catalyst; (f) 10% Pd/C, 1 atm of H$_2$.

Table 2. Cyclic Voltammetry Data[a]

complex	$E_{p/a}$ [V]	$E_{p/c}$ [V]	$E°$ [V]	ΔE [mV]	$i_{c/a}$
4b	1.306	1.237	1.271	76	0.54
4c	1.314	1.245	1.279	75	0.54
8a	1.298	1.221	1.260	77	0.65
8b	1.314	1.251	1.283	63	0.55
8c	1.319	1.214	1.272	105	0.43
8d	1.305	1.208	1.256	97	0.53
11a	1.306	1.224	1.265	82	0.78
11b	1.298	1.222	1.260	76	0.80
11c	1.318	1.261	1.289	77	0.73
11d	1.300	1.236	1.268	63	0.82
14c	1.465	1.372	1.418	93	0.35
14d	1.444	1.357	1.400	88	0.37

[a] Conditions: (7−9) × 10^{-4} M, *n*-Bu$_4$N$^+$ BF$_4^-$/CH$_2$Cl$_2$ at 22.5 ± 1 °C; Pt working and counter electrodes, potential vs Ag wire pseudoreference; scan rate 100 mV s^{-1}; ferrocene = 0.46 V.

these higher-temperature processes are beyond the scope of the present study.

Finally, low temperature ^{1}H and ^{13}C NMR spectra of **11b**−**d** and **14d** were recorded in CD_2Cl_2 and $CDFCl_2$ under conditions similar to those used for related compounds in the preceding paper.[9] No decoalescence phenomena were observed.

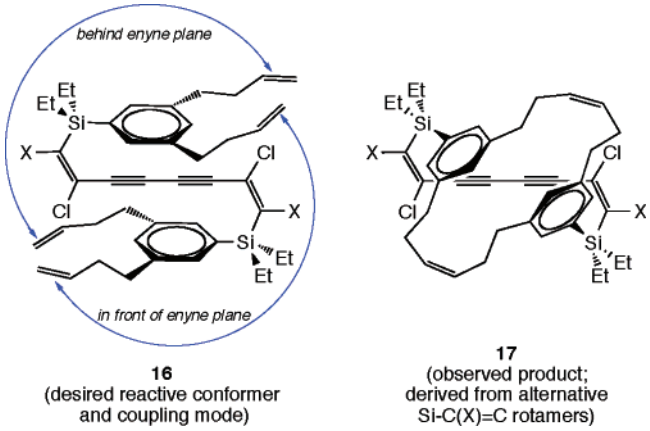

Figure 4. Other approaches to shielded polyynes involving alkene metathesis.

Discussion

1. Syntheses. Schemes 4 and 5 establish a new strategy for sterically shielding unsaturated assemblies that connect two electroactive groups,[27−30] complementing that in the preceding paper.[9] Related efforts in other laboratories have featured cyclophane[27a−d,29] and cyclodextrin[27e] derived rotaxanes, and dendrimers.[28] However, prior to this work, no approaches involving alkene metathesis had been attempted. The success of Schemes 4 and 5 hinges upon three factors that could not be taken for granted in advance: (1) the ability to oxidatively couple Pt(C≡C)$_{n/2}$H species in the presence of pendant vinyl groups; (2) the ability of Grubbs' catalyst to metathesize terminal alkene moieties in the presence of Pt(C≡C)$_n$Pt linkages and 16-valence-electron metal centers; (3) the ability to hydrogenate disubstituted alkenes in the presence of Pt(C≡C)$_n$Pt linkages.

Recently, a conceptually related approach to sterically shielding polyynes was investigated, using the silicon-substituted diyne **16** shown in Figure 4.[31] Each silicon features an aryl group with two meta-disposed (CH$_2$)$_2$CH═CH$_2$ substituents. In principle, a twofold intramolecular alkene metathesis could "sandwich" the diyne segment between the aryl groups (arrows). However, an alternative *Si*−*C*(X)═C conformer proved more reactive, and only **17**, in which one side of the diyne is shielded, was isolated.

Figure 4 leads into an obvious question regarding the ring closure selectivities in Schemes 4 and 5. First, products with termini-spanning diphosphine ligands dominate over those with *trans*-spanning diphosphine ligands (**11** vs **8** and **14** vs **15**). However, given the oligomeric byproducts and presence of *E*/*Z* C═C isomers prior to hydrogenation, more exact *in situ* analyses

(27) (a) Anderson, S.; Aplin, R. T.; Claridge, T. D. W.; Goodson T., III; Maciel, A. C.; Rumbles, G.; Ryan, J. F.; Anderson, H. L. *J. Chem. Soc., Perkin Trans. 1* **1998**, 2383. (b) Taylor, P. N.; O'Connell, M. J.; McNeill, L. A.; Hall, M. J.; Aplin, R. T.; Anderson, H. L. *Angew. Chem., Int. Ed.* **2000**, *39*, 3456; *Angew. Chem.* **2000**, *112*, 3598. (c) Buston, J. E. H.; Marken, F.; Anderson, H. L. *J. Chem. Soc., Chem. Commun.* **2001**, 1046. (d) Taylor, P. N.; Hagan, A. J.; Anderson, H. L. *Org. Biomol. Chem.* **2003**, *1*, 3851. (e) Michels, J. J.; O'Connell, M. J.; Taylor, P. N.; Wilson, J. S.; Cacialli, F.; Anderson, H. L. *Chem.—Eur. J.* **2003**, *9*, 6167. (f) Terao, J.; Tang, A.; Michels, J. J.; Krivokapic, A.; Anderson, H. L. *Chem. Commun.* **2004**, 56. (g) Klotz, E. J. F.; Claridge, T. D. W.; Anderson, H. L. *J. Am. Chem. Soc.* **2006**, *128*, 15374.
(28) Schenning, A. P. H. J.; Arndt, J.-D.; Ito, M.; Stoddart, A.; Schreiber, M.; Siemsen, P.; Martin, R. E.; Boudon, C.; Gisselbrecht, J.-P.; Gross, M.; Gramlich, V.; Diederich, F. *Helv. Chim. Acta* **2001**, *84*, 296.
(29) (a) Lee, D.; Swager, T. M. *Synlett* **2004**, 149. (b) Kwan, P. H.; Swager, T. M. *Chem. Commun.* **2005**, 5211.
(30) Li, C.; Numata, M.; Bae, A.-H.; Sakurai, K.; Shinkai, S. *J. Am. Chem. Soc.* **2005**, *127*, 4548.
(31) Simpkins, S. M. E.; Kariuki, B. M.; Cox, L. R. *J. Organomet. Chem.* **2006**, *691*, 5517.

are not feasible. The combination of 8 and 16 sp and sp^3 carbon atoms (**11b**) appears particularly favorable for termini-spanning diphosphine ligands. Complexes with oxygen-containing $P(CH_2)_2O(CH_2)_2CH{=}CH_2$ linkages give analogous selectivities.[11b,13] However, analogues with geminal dimethyl groups can exhibit opposite selectivities.[12b,13]

The good yields of monoplatinum complexes with *trans*-spanning diphosphine ligands in Scheme 3 (**5a**,**b**) underscore the viability of this ring-closure mode. We have conducted many other types of ring closing alkene metatheses in the coordination spheres of platinum(II) complexes[16,17a,32,33] and, in most cases, believe that the product distributions are kinetic or, at a minimum, that not all possible products have been thermodynamically sampled. Only in a few cases, involving smaller rings and Grubbs' second generation catalyst, has it been possible to equilibrate monomers and oligomers.[32,34] Hence, there remains the possibility that catalytic conditions that promote higher turnover numbers may give altered selectivities.

The stabilities of the title complexes with respect to oligomerization has implications for the reactions of *trans*,*trans*-$(C_6F_5)(p\text{-}tol_3P)_2Pt(C{\equiv}C)_nPt(Pp\text{-}tol_3)_2(C_6F_5)$ and $Ar_2P(CH_2)_m$-PAr_2 in the preceding paper. In some of the cases where oligomers are isolated (n/m = 4/≥16, 6/≥19), NMR signals corresponding to the target molecules can be detected prior to concentration of the reaction mixture. This suggests that oligomerization is promoted by some species present. In our opinion, likely candidates would include the displaced phosphine $Pp\text{-}tol_3$ as well as any excess $Ar_2P(CH_2)_mPAr_2$. However, mechanistic investigations are beyond the scope of our present work.

2. Crystal Structures. Of the new structures in Figures 1−3, four contain *trans*-spanning diphosphine ligands. We have previously reported the syntheses and structures of a variety of such *mono*platinum complexes with C_6F_5PtCl moieties (e.g., **5a**,**c**,**d**).[16,17a,21] Complex **7b** (Figure 2) represents an analogue that features both a new ligand (trimethylsilylbutadienyl) and macrocycle size (19). It exhibits the usual aryl/C_6F_5/aryl stacking motif.

As noted above, the diplatinum complexes **8a**,**c**,**d** crystallize in "double half-clamshell" conformations (Figure 1). The periphery of the clamshell is best viewed from a plane perpendicular to that of the C_6F_5 ligand, as shown in **I**, **J**, and **K**. As the number of sp^3 carbon atoms increases from 14 to 18 to 20, the periphery extends further from the platinum atom, shifting the line-of-sight to the sp chain. The average distances of the sp^3 carbon atoms from the platinum−platinum vector also increase slightly (4.12, 4.20, 4.21 Å). At the same time, the methylene groups occupy increasing amounts of space above and below the planes of the C_6F_5 ligands, until saturation is achieved with **8d** (compare **L**, **M**, **N**). The net result is a marked increase in the steric shielding of the sp chain.

The crystal structure of **8a**·EtOH can be compared with those of two solvates of the double-helical isomer **11a** in the preceding paper.[9] When viewed from perspectives such as **I** and **L**, the steric shielding of the sp carbon chain is much less extensive. The average distance of the sp^3 carbon atoms from the platinum−platinum vector is also considerably greater (4.12 vs 4.05−3.98 Å). The crystal structure of **8d** can similarly be compared to that of the helical isomer **11d** (Figure 3, top). Again, the steric shielding is not as extensive, and the sp^3 carbon atoms are further removed from the sp chain (4.21 vs 4.13 Å).

The crystal structure of **11d** is remarkable for the extensive degree of twisting between the endgroups (294.8°). This is significantly greater than that in four lower homologues with diphosphines of the formula $Ar_2P(CH_2)_{14}PAr_2$ in the preceding paper (189.9°−196.6°). Hence, increasing the length of the sp^3 carbon chain can markedly increase helicity. However, the increased average distance of the sp^3 carbon atoms from the platinum−platinum vector in **11d** (4.13 vs 3.76−3.90 Å) hints at a possible limit. As the sp^3 chains become longer, the contact surface of the sp chain will eventually be saturated, requiring helices of greater radii or alternative conformations.[35]

The sp^3 chains in both **11d** and **14d** contain 20 carbon atoms. However, the crystal structure of the latter (Figure 3, bottom) exhibits a nonhelical conformation. Although this can be rationalized from the increased sp chain length (12 vs 8 carbon atoms), the structural data for the lower homologue **14c**, which exhibits both helical and nonhelical molecules in the unit cell, had led us to anticipate a helical structure. Unfortunately, crystals of the higher homologue **14e** could not be obtained. Nonetheless, we view analogues with sp^3 chains of 24 to 36 carbon atoms as particularly promising for highly coiled double-helical structures, and synthetic efforts remain underway.

3. Spectroscopic, Redox, and Dynamic Properties. In principle, the new complexes **11b**−**d** and **14d**,**e** allow the effect of longer sp^3 carbon chains upon the spectroscopic properties of the title molecules to be defined. In practice, and as with the shorter sp^3 chains, all data are very similar to those of $Pt(C{\equiv}C)_nPt$ complexes that lack termini-spanning diphosphine ligands. The uncyclized monophosphine complexes **4a**−**d** and **13c**−**e** also constitute useful reference compounds. Tables that compare IR and NMR data are supplied in the Supporting Information. The most pronounced trend is a slight downfield shift of the Pt*C*≡ ^{13}C NMR signal in the series **11a**−**c** (98.6, 99.3, 101.0 ppm).

A related question involves the relative spectroscopic properties of complexes with termini- and *trans*-spanning diphosphine ligands, such as **11** vs **8**. As noted above, the mass spectra exhibit significant differences. However, the IR and UV−visible spectra are identical, as tabulated in the Supporting Information. The Pt*C*≡*CC*≡*C* and P*CH*$_2$*CH*$_2$*CH*$_2$ ^{13}C NMR chemical shifts all fall into narrow ranges. Of the latter group, the $PCH_2CH_2CH_2$ (31.7−30.6 ppm) and P*CH*$_2$ (28.5−27.9 ppm) signals are the furthest downfield (PCH_2CH_2, 26.6−25.6 ppm). Interestingly, **11a**−**d** always exhibit more CH_2 signals with chemical shifts

(32) Shima, T.; Bauer, E. B.; Hampel, F.; Gladysz, J. A. *Dalton Trans.* **2004**, 1012.
(33) Nawara, A. J.; Shima, T.; Hampel, F.; Gladysz, J. A. *J. Am. Chem. Soc.* **2006**, *128*, 4962.
(34) Shima, T.; Hampel, F.; Gladysz, J. A. *Angew. Chem., Int. Ed.* **2004**, *43*, 5537; *Angew. Chem.* **2004**, *116*, 5653.

(35) As tabulated in the Supporting Information, there are seven gauche segments in the one non-disordered sp^3 chain of **11d**, as opposed to three to four in each sp^3 chain of the four $Ar_2P(CH_2)_{14}PAr_2$ homologues. However, near one terminus, two are of the opposite sign. We intuit this situation as follows. If the endgroup planes were twisted to the maximum degree allowed by the sp^3 chain lengths, all gauche segments should have the same helical chirality. Short of this limit, there is "play" in the sp^3 chains, as reflected by a greater average sp^3/sp chain distance. Thus, the gauche segments can "overshoot" the plane of the endgroup and, by necessity, must "double back", resulting in two chirality domains. This feature is also found in one sp^3 chain of one of the four $Ar_2P(CH_2)_{14}PAr_2$ homologues, **11a**·$(benzene)_{1.5}$.[9] The average sp^3/sp distance is greater than that of the pseudopolymorph **11a**·$(toluene)_{1.5}$ (4.05 vs. 3.98 Å), in which the gauche torsion angles have the same sign.

between those of the $PCH_2CH_2CH_2$ and PCH_2 signals than **8a**−**d**. This suggests, in accord with established shielding trends,[36] a small but detectable downfield shift of the sp^3 carbon atoms that run along the sp chain.

As analyzed in the preceding paper, the $i_{c/a}$ and ΔE values obtained by cyclic voltammetry (Table 2) are presumed to reflect the relative stabilities of the corresponding radical cations.[9] Complexes **4b**,**c**, which contain monophosphine ligands with potentially reactive vinyl groups and sp carbon chains that are quite exposed, exhibit relatively low $i_{c/a}$ values (0.54). The complexes **8a**−**d**, with *trans*-spanning diphosphine ligands, are on the average similar (0.43−0.65). However, the double-helical complexes **11a**−**d** give significantly higher values (0.73−0.82), consistent with enhanced radical cation stabilities. The oxidation of the most highly coiled **11d** exhibits the highest degree of reversibility (ΔE 63 mV; $i_{c/a}$ 0.82).

Although oxidations of the dodecahexaynediyl complexes **14c**,**d** are poorly reversible ($i_{c/a}$ 0.35−0.37), this represents an improvement over nonshielded analogues.[14a] The more positive $E°$ values for **14c**,**d** indicate thermodynamically more difficult oxidations. This chain length effect is general for all polyynediyl complexes, and the origin has been defined by computational studies.[37]

Unfortunately, low-temperature NMR spectra of **11b**−**d** and **14d** did not show any decoalescence phenomena. A chiral double-helical structure (**A**, Scheme 1) should give separate signals for various diastereotopic groups, providing that interconversion with the enantiomer is slow on the NMR time scale. Thus, despite the many helical crystal structures, other possibilities cannot be excluded for the dominant conformation of the title molecules in solution. Nonetheless, we remain optimistic that barriers should increase into a measurable regime with longer sp and sp^3 carbon chains. Hence, higher homologues of **14c**−**e** with additional methylene groups remain under active pursuit.

Additional approaches to increasing the barrier for enantiomer interconversion are readily identified. Possibilities include introducing (a) functional groups into the sp^3 chain that might have attractive interactions with the sp chains or (b) groups that could raise barriers to the sp^3−sp^3 carbon−carbon bond rotations necessary to convert gauche conformational segments into their enantiomers. Our initial efforts with the former have been communicated,[11b] and both will be detailed in subsequent full papers.[13]

Conclusion

This paper has established the viability of alkene metatheses in platinum coordination spheres, together with other reactions with little if any precedent, for the construction of novel sterically shielded polyynediyl complexes of the types **A**−**C** (Scheme 1). These sequences significantly advance the art of organometallic chemistry with respect to rational, directed syntheses of new metal-containing materials. With a single exception, all complexes of the types **A/B** with sufficiently long methylene chains crystallize in double-helical conformations. Similar conformations are thought to dominate in solution, but conclusive data have proved elusive, presumably due to low barriers for interconversion of the enantiomers. Accordingly, future papers will detail efforts directed at analogous compounds with functional modifications of the sp^3 chain that have the potential to raise these barriers.[13]

Experimental Section[38]

***trans*-$(C_6F_5)(Ph_2P(CH_2)_6CH{=}CH_2)_2Pt(C{\equiv}C)_2H$ (3a).** A Schlenk flask was charged with *trans*-$(C_6F_5)(Ph_2P(CH_2)_6CH{=}CH_2)_2PtCl$ (**1a**;[16] 0.830 g, 0.838 mmol), CuI (0.033 g, 0.18 mmol), CH_2Cl_2 (5.4 mL), and $HNEt_2$ (54 mL) with stirring and cooled to −45 °C. Then $H(C{\equiv}C)_2H$ (15.8 mL, 13.4 mmol, ca. 2.4 M in THF)[39] was added, and the mixture turned light yellow. The cold bath was allowed to warm to 10 °C over the course of 3 h and was then removed. After an additional 2.5 h (orange supernatant/white precipitate), the solvent was removed by oil pump vacuum. The tan residue was extracted with toluene (3 × 3 mL). The combined extracts were filtered through an alumina column (4 cm × 2.5 cm), which was eluted with toluene. The solvent was removed from the filtrate/washings by oil pump vacuum to give **3a** as a yellow-tan oil (0.746 g, 0.743 mmol, 89%). Calcd for $C_{50}H_{51}F_5P_2Pt$: C: 59.82; H: 5.12. Found: C: 59.77; H: 5.11.

NMR (δ, $CDCl_3$) ^1H 7.41 (m, 8H of 4 Ph), 7.27 (m, 4H of 4 Ph), 7.20 (m, 8H of 4 Ph), 5.81−5.73 (m, 2H, CH═), 4.99−4.88 (m, 4H, $═CH_2$), 2.52 (m, 4H, PCH_2), 1.97 (m, 4H, $CH_2CH{=}$), 1.72 (m, 4H, PCH_2CH_2), 1.38−1.26 (m, 12H, remaining CH_2); $^{13}C\{^1H\}$[40,41] 146.5 (d, $^1J_{CF}$ = 235 Hz, *o* to Pt), 139.2 (s, CH═), 136.5 (dm, $^1J_{CF}$ = 240 Hz, *m*/*p* to Pt), 133.2 (virtual t, $^2J_{CP}$ = 5.5 Hz, *o* to P), 131.9 (virtual t, $^1J_{CP}$ = 26.7 Hz, *i* to P), 130.4 (s, *p* to P), 128.1 (virtual t, $^3J_{CP}$ = 5.5 Hz, *m* to P), 114.4 (s, $═CH_2$), 92.4 (s, PtC≡*C*), 72.4 (s, PtC≡C*C*), 59.8 (s, PtC≡CC≡*C*), 33.8 (s, $CH_2CH{=}$), 31.2 (virtual t, $^3J_{CP}$ = 7.5 Hz, $PCH_2CH_2CH_2$), 28.8 (s, CH_2), 28.6 (s, CH_2), 28.2 (virtual t, $^1J_{CP}$ = 17.5 Hz, PCH_2), 25.5 (s, PCH_2CH_2); $^{31}P\{^1H\}$ 15.5 (s, $^1J_{PPt}$ = 2568 Hz).[42]

IR (cm^{-1}, oil film) $\nu_{{\equiv}CH}$ 3308 (w), $\nu_{C{\equiv}C}$ 2150 (m). MS:[43] 1005 ([**3a**$^+$, 3%), 954 ([**3a**−$C_4H]^+$, 10%), 785 ([**3a**−C_4H−$C_6F_5]^+$, 8%), 489 ([Pt-$(Ph_2P(CH_2)_6CH{=}CH_2)]^+$, 60%), 297 ([$Ph_2P(CH_2)_6CH{=}CH_2]^+$, 100%).

***trans,trans*-$(C_6F_5)(Ph_2P(CH_2)_6CH{=}CH_2)_2Pt(C{\equiv}C)_4Pt(Ph_2P$-$(CH_2)_6CH{=}CH_2)_2(C_6F_5)$ (4a).** A three-necked flask was charged with **3a** (0.400 g, 0.398 mmol) and acetone (10 mL) and fitted with a gas inlet needle and a condenser chilled via circulating −18 °C ethanol.[44] A Schlenk flask was charged with CuCl (0.050 g, 0.51 mmol) and acetone (15 mL), and TMEDA (0.020 mL, 0.13 mmol) was added with stirring. After 0.5 h, stirring was halted (blue supernatant/yellow-green solid). Then O_2 was bubbled through the three-necked flask with stirring, and the solution heated to 65 °C. The blue supernatant was added in portions over 1.5 h. After an additional 0.5 h, the solvent was removed by rotary evaporation and oil pump vacuum. Toluene was added (2 × 3 mL), and the mixture was transferred to an alumina column (4 cm × 2.5 cm), which was rinsed with toluene until UV monitoring (fluorescence of spotted TLC plate) showed no absorbing material (ca. 30 mL).

(36) Wannere, C. S.; Schleyer, P. v. R. *Org. Lett.* **2003**, *5*, 605.
(37) Zhuravlev, F.; Gladysz, J. A. *Chem.—Eur. J.* **2004**, *10*, 6510.

(38) A representative procedure for each type of transformation and all metathesis/hydrogenation sequences involving diplatinum complexes that afford a pure product are described in the text. All other syntheses are detailed in the Supporting Information.
(39) Verkruijsse, H. D.; Brandsma, L. *Synth. Commun.* **1991**, *25*, 657. The $H(C{\equiv}C)_2H$ concentration is calculated from the mass increase of the THF solution. **CAUTION**: this compound is explosive and literature precautions should be followed.
(40) (a) In some ^{13}C NMR spectra, the PtC≡ signal or certain C_6F_5 signals were not observed. (b) For virtual triplets (Hersh, W. H. *J. Chem. Educ.* **1997**, *74*, 1485), the *J* values represent the *apparent* couplings between adjacent peaks. (c) The PtC≡CC≡C signals were assigned according to trends established earlier.[14]
(41) Complexes with $PtPCH_2CH_2CH_2$ linkages exhibit a characteristic pattern of ^{13}C signals. The signals were assigned by analogy to related platinum complexes as described in the previous[9] and following[13] full papers in this series.
(42) This coupling represents a satellite (d; ^{195}Pt = 33.8%) and is not reflected in the peak multiplicity given.
(43) FAB (3-nitrobenzyl alcohol matrix); *m*/*z* for the most intense peak of the isotope envelope; relative intensities are for the specified mass range.
(44) Without a chilled condenser, aspirated acetone must be replenished during the reaction.

The solvent was removed by rotary evaporation and oil pump vacuum to give **4a** as a tan oil (0.335 g, 0.167 mmol, 84%). Calcd for $C_{100}H_{100}F_{10}Pt_2P_4$: C, 59.88; H, 5.02. Found: C, 59.85; H, 5.39.

NMR (δ, $CDCl_3$) ^{1}H 7.45 (m, 16H of 8 Ph), 7.31 (m, 8H of 8 Ph), 7.24 (m, 16H of 8 Ph), 5.83−5.72 (m, 4H, CH═), 4.99−4.87 (m, 8H, ═CH_2), 2.55 (m, 8H, PCH_2), 2.01 (m, 8H, CH_2CH═), 1.75 (m, 8H, PCH_2CH_2), 1.42−1.26 (m, 24H, remaining CH_2); $^{13}C\{^1H\}$[40,41] 146.1 (dm, $^1J_{CF}$ = 230 Hz, *o* to Pt), 139.1 (s, CH═), 136.5 (dm, $^1J_{CF}$ = 245 Hz, *m*/*p* to Pt), 133.0 (virtual t, $^2J_{CP}$ = 5.8 Hz, *o* to P), 131.5 (virtual t, $^1J_{CP}$ = 28.0 Hz, *i* to P), 130.3 (s, *p* to P), 127.9 (virtual t, $^3J_{CP}$ = 5.2 Hz, *m* to P), 114.4 (s, ═CH_2), 94.2 (s, PtC≡*C*), 63.7 (s, PtC≡C*C*), 58.0 (s, PtC≡CC≡*C*), 33.8 (s, CH_2CH═), 31.2 (virtual t, $^3J_{CP}$ = 7.7 Hz, $PCH_2CH_2CH_2$), 28.8 (s, CH_2), 28.6 (s, CH_2), 28.2 (virtual t, $^1J_{CP}$ = 17.9 Hz, PCH_2), 25.4 (s, PCH_2CH_2); $^{31}P\{^1H\}$ 14.2 (s, $^1J_{PPt}$ = 2565 Hz).[42]

IR (cm^{-1}, oil film) $\nu_{C\equiv C}$ 2150 (m), 2003 (w). UV−vis:[45] 291 (66 400), 320 (81 600), 355 (7200), 381 (4000), 411 (2400). MS:[43] 2005 (**4a**$^+$, 20%), 954 ($[(C_6F_5)Pt(Ph_2P(CH_2)_6CH$═$CH_2)_2]^+$, 100%).

***trans*-(C_6F_5)(Ph_2P(CH_2)$_{16}$$Ph_2$P)Pt($C\equiv C)_2SiMe_3$ (7b).** A Schlenk flask was charged with **5b** (0.223 g, 0.225 mmol), $Me_3Sn(C\equiv C)_2SiMe_3$ (0.077 g, 0.27 mmol),[19] CuI (0.0086 g, 0.0045 mmol), KPF_6 (0.049 g, 0.27 mmol), CH_2Cl_2 (4 mL), and methanol (4 mL) with stirring. After 16 h, the solvent was removed by oil pump vacuum. The residue was chromatographed on an alumina column (7 cm × 2 cm, 90:10 v/v hexanes/CH_2Cl_2). The solvent was removed from the product-containing fractions by oil pump vacuum to give **7b** as a white powder (0.191 g, 0.177 mmol, 79%), mp 171 °C. Calcd for $C_{53}H_{61}F_5P_2PtSi$: C, 59.04; H, 5.70. Found: C, 58.75; H, 5.70. DSC:[46] endotherm with T_i, 45.2 °C; T_e, 51.9 °C; T_p, 55.6 °C; T_c, 58.1 °C; T_f, 62.9 °C; exotherm with T_i, 66.3 °C; T_e, 78.2 °C; T_p, 86.5 °C; T_c, 90.8 °C; T_f, 106.4 °C; endotherm with T_i, 153.3 °C; T_e, 174.9 °C; T_p, 176.5 °C; T_c, 177.9 °C; T_f, 199.7 °C. TGA: weight loss 36%, 230−396 °C.

NMR (δ, $CDCl_3$) ^{1}H 7.79−7.77 (m, 4H of 4 Ph), 7.45−7.39 (m, 6H of 4 Ph), 7.17−7.10 (m, 2H of 4 Ph), 7.08−7.05 (m, 8H of 4 Ph), 2.81−2.77 (m, 2H, PC*H*H′), 2.63−2.59 (m, 2H, PCH*H*′), 2.18−2.16 (m, 2H, PCH_2CHH′), 1.86−1.84 (m, 2H, PCH_2CH*H*′), 1.55−1.32 (m, 24H, remaining CH_2), 0.09 (s, 9H, $SiCH_3$); $^{13}C\{^1H\}$[40,41] 146.5 (dm, $^1J_{CF}$ = 221 Hz, *o* to Pt), 136.3 (dm, $^1J_{CF}$ = 235 Hz, *m*/*p* to Pt), 134.4 (virtual t, $^2J_{CP}$ = 6.3 Hz, *o* to P), 132.0 (virtual t, $^1J_{CP}$ = 26.8 Hz, *i* to P), 131.7 (virtual t, $^2J_{CP}$ = 5.2 Hz, *o* to P), 131.4 (virtual t, $^1J_{CP}$ = 28.3 Hz, *i* to P), 130.0 (s, *p* to P), 129.0 (s, *p* to P), 128.2 (virtual t, $^3J_{CP}$ = 5.4 Hz, *m* to P), 128.0 (virtual t, $^3J_{CP}$ = 5.9 Hz, *m* to P), 99.1 (s, PtC≡), 93.8, 92.4, 76.8 (3 s, PtC≡*CC*≡*C*), 30.8 (virtual t, $^3J_{CP}$ = 7.7 Hz, PCH_2-CH_2CH_2), 28.3 (virtual t, $^1J_{CP}$ = 18.2 Hz, PCH_2), 28.1 (s, CH_2), 27.9 (s, 2 CH_2), 27.6 (s, CH_2), 27.4 (s, CH_2), 25.4 (s, PCH_2CH_2), 0.9 (s, $SiCH_3$); $^{31}P\{^1H\}$ 14.3 (s, $^1J_{PPt}$ = 2586 Hz).[42]

IR (cm^{-1}, powder film) $\nu_{C\equiv C}$ 2181 (w), 2131 (m). MS:[43] 1079 (**7b**$^+$, 100%), 956 ([**7b**−C_2SiMe_3]$^+$, 40%), 787 ([**7b**−C_2SiMe_3−C_6F_5]$^+$, 90%).

***trans,trans*-(C_6F_5)(Ph_2P(CH_2)$_{14}$$PPh_2$)Pt($C\equiv C)_4$Pt($PPh_2$($CH_2$)$_{14}$$PPh_2$)-($C_6F_5$) (8a).** Complex **6a** (0.060 g, 0.062 mmol), acetone (5 mL), CuCl (0.050 g, 0.51 mmol), acetone (15 mL), TMEDA (0.020 mL, 0.13 mmol), and O_2 were combined in a procedure analogous to that for **4a**. An identical workup gave **8a** as a yellow powder (0.050 g, 0.076 mmol, 84%), dec pt. > 208 °C (gradual darkening without melting). Calcd for $C_{96}H_{96}F_{10}P_4Pt_2$: C, 59.02; H, 4.95. Found: C, 59.44; H, 5.46. DSC:[46] endotherm with T_i, 183.2 °C; T_e, 210.1 °C; T_p, 215.3 °C; T_c, 224.0 °C; T_f, 230.2 °C. TGA: onset of mass loss, 264.1 °C (T_e).

NMR (δ, $CDCl_3$) ^{1}H 7.85−7.83 (m, 8H of 8 Ph), 7.46−7.40 (m, 12H of 8 Ph), 7.12−6.96 (m, 20H of 8 Ph), 2.73−2.66 (m, 4H, PC*H*H′), 2.66−2.56 (m, 4H, PCH*H*′), 2.18−2.15 (m, 4H, PCH_2CH*H*′), 1.86 (m, 4H, PCH_2CHH′), 1.52−1.11 (m, 40H, remaining CH_2); $^{13}C\{^1H\}$[40,41] 145.5 (dm, $^1J_{CF}$ = 233 Hz, *o* to P), 136.3 (dm, $^1J_{CF}$ = 258 Hz, *m*/*p* to Pt), 134.7 (virtual t, $^2J_{CP}$ = 6.5 Hz, *o* to P), 132.2 (virtual t, $^1J_{CP}$ = 27.4 Hz, *i* to P), 131.4 (virtual t, $^1J_{CP}$ = 28.5 Hz, *i* to P), 131.0 (virtual t, $^2J_{CP}$ = 5.4 Hz, *o* to P), 130.95 (s, *p* to P), 129.5 (s, *p* to P), 128.3 (virtual t, $^3J_{CP}$ = 5.3 Hz, *m* to P), 127.5 (virtual t, $^3J_{CP}$ = 4.6 Hz, *m* to P), 94.2 (s, PtC≡*C*), 63.8 (s, PtC≡C*C*), 58.4 (s, PtC≡CC≡*C*), 30.9 (virtual t, $^3J_{CP}$ = 8.1 Hz, $PCH_2CH_2CH_2$), 28.6 (virtual t, $^1J_{CP}$ = 17.9 Hz, PCH_2), 27.6 (s, CH_2), 27.5 (s, CH_2), 27.2 (s, CH_2), 26.3 (s, CH_2), 25.8 (s, PCH_2CH_2); $^{31}P\{^1H\}$ 14.7 (s, $^1J_{PPt}$ = 2576 Hz).[42]

IR (cm^{-1}, powder film) $\nu_{C\equiv C}$ 2142 (m), 1998 (w). MS:[43] 1954 (**8a**$^+$, 26%), 1786 ([**8a**−C_6F_5]$^+$, <2%), 928 ($[(C_6F_5)Pt(PPh_2(CH_2)_{14}PPh_2)]^+$, 100%), 759 ($[Pt(PPh_2(CH_2)_{14}PPh_2)]^+$, 40%)

***trans,trans*-(C_6F_5)(Ph_2P(CH_2)$_{16}$$PPh_2$)Pt($C\equiv C)_4$Pt($Ph_2$P($CH_2$)$_{16}$$PPh_2$)-($C_6F_5$) (8b).** A three-necked flask was charged with **7b** (0.209 g, 0.194 mmol) and acetone (10 mL) and fitted with a gas inlet needle and a condenser chilled via circulating −18 °C ethanol.[44] A Schlenk flask was charged with CuCl (0.100 g, 1.01 mmol) and acetone (15 mL), and TMEDA (0.200 mL, 1.20 mmol) was added with stirring. After 0.5 h, stirring was halted (blue supernatant/yellow-green solid). Then *n*-Bu_4N^+ F^- (0.039 mL, 0.039 mmol, 1 M in THF/5 wt % H_2O) was added to the solution of **7b** with stirring. After 20 min, Me_3SiCl (0.024 mL, 0.19 mmol) was added. Then O_2 was bubbled through the three-necked flask with stirring, and the solution heated to 65 °C. The blue supernatant was added in portions over 4 h. After an additional 0.5 h, the solvent was removed by oil pump vacuum. The residue was extracted with hexanes (2 × 5 mL) and then toluene (3 × 5 mL). The extracts were filtered in sequence through an alumina column (4 cm × 2 cm), which was rinsed with toluene. The solvent was removed from the toluene fractions by rotary evaporation and oil pump vacuum. The residue was chromatographed on a silica gel column (10 cm × 1 cm, 70:30 v/v hexanes/CH_2Cl_2). The solvent was removed from the product-containing fractions by oil pump vacuum to give **8b** as a yellow powder (0.176 g, 0.0878 mmol, 90%), dec pt. > 207 °C (gradual darkening without melting). Calcd for $C_{100}H_{104}F_{10}P_4Pt_2$: C, 59.76; H, 5.22. Found: C, 58.94; H, 5.22. DSC:[46] endotherm with T_i, 112.5 °C; T_e, 126.5 °C; T_c, 131.9 °C; T_f, 154.3 °C; endotherm with T_i, 174.4 °C; T_e, 182.9 °C; T_c, 186.4 °C; T_f, 188.7 °C; endotherm with T_i, 200.6 °C; T_e, 217.4 °C; T_c, 219.7 °C; T_f, 230.2 °C. TGA: weight loss 33%, 243−414 °C.

NMR (δ, $CDCl_3$) ^{1}H 7.80−7.76 (m, 8H of 8 Ph), 7.44−7.37 (m, 12H of 8 Ph), 7.15−7.14 (m, 4H of 8 Ph), 7.06−7.03 (m, 16H of 8 Ph), 2.69−2.57 (m, 8H, PCH_2), 2.10−2.06 (m, 4H, PCH_2CH*H*′), 1.86−1.84 (m, 4H, PCH_2CHH′), 1.55−1.29 (m, 48H, remaining CH_2); $^{13}C\{^1H\}$[40,41] 145.8 (dm, $^1J_{CF}$ = 248 Hz, *o* to Pt), 136.3 (dm, $^1J_{CF}$ = 260 Hz, *m*/*p* to Pt), 134.5 (virtual t, $^2J_{CP}$ = 6.3 Hz, *o* to P), 132.0 (virtual t, $^1J_{CP}$ = 26.8 Hz, *i* to P), 131.3 (virtual t, $^2J_{CP}$ = 5.3 Hz, *o* to P), 131.1 (virtual t, $^1J_{CP}$ = 28.2 Hz, *i* to P), 130.8 (s, *p* to P), 129.5 (s, *p* to P), 128.2 (virtual t, $^3J_{CP}$ = 5.4 Hz, *m* to P), 127.5 (virtual t, $^3J_{CP}$ = 4.7 Hz, *m* to P), 99.4 (s, PtC≡), 92.3 (s, PtC≡*C*), 63.7 (s, PtC≡C*C*), 58.4 (s, PtC≡CC≡*C*), 31.1 (virtual t, $^3J_{CP}$ = 7.7 Hz, $PCH_2CH_2CH_2$), 28.4 (virtual t, $^1J_{CP}$ = 18.2 Hz, PCH_2), 28.4 (s, CH_2), 28.2 (s, CH_2), 28.1 (s, CH_2), 27.4 (s, CH_2), 27.1 (s, CH_2), 25.8 (s, PCH_2CH_2); $^{31}P\{^1H\}$ 14.4 (s, $^1J_{PPt}$ = 2576 Hz).[42]

IR (cm^{-1}, powder film) $\nu_{C\equiv C}$ 2146 (m), 2003 (w). UV−vis:[45] 263 (88 000), 291 (105 000), 321 (130 000), 353 (6200), 379 (5000), 410 (2700). MS:[43] 2009 (**8b**$^+$, 45%), 956 ($[(C_6F_5)Pt(Ph_2P(CH_2)_{16}PPh_2)]^+$, 100%), 785 ($[Pt(Ph_2P(CH_2)_{16}PPh_2)]^+$, 70%).

Alkene Metathesis of 4a. A two-necked flask was charged with Grubbs' catalyst (ca. half of 0.008 g, 0.01 mmol), **4a** (0.299 g, 0.149 mmol), and CH_2Cl_2 (140 mL) with stirring and fitted with a condenser. The solution was refluxed. After 2 h, the remaining catalyst was added. After 3 h, the solvent was removed by rotary evaporation and oil pump vacuum to give a tan solid. Then CH_2Cl_2 was added (2 × 3 mL), and

(45) UV−visible spectra were recorded in CH_2Cl_2 (1.25×10^{-5} M unless noted). Absorptions are in nm (ϵ, M^{-1} cm^{-1}).

(46) (a) DSC and TGA data were treated as recommended by: Cammenga, H. K.; Epple, M. *Angew. Chem., Int. Ed. Engl.* **1995**, *34*, 1171; *Angew. Chem.* **1995**, *107*, 1284. The T_e values best represent the temperature of the phase transition or exotherm. (b) Except in cases of desolvation, DSC measurements were not continued beyond the onset of mass loss (TGA).

the sample was transferred to an alumina column (4 cm × 2.5 cm). The column was eluted with CH_2Cl_2 until UV monitoring showed no absorbing material (ca. 30 mL). The solvent was removed by rotary evaporation and oil pump vacuum to give a mixture of cyclized products as a tan solid (0.280 g, 0.144 mmol, 96%). Calcd for $C_{96}H_{92}F_{10}P_4Pt_2$: C, 59.14; H, 4.76. Found: C, 58.99; H, 4.86.

NMR (δ, $CDCl_3$) ^{1}H 7.90 (m, 6H of 8 Ph), 7.48−6.89 (m, 34H of 8 Ph), 5.37−5.35 (m, 4H, C*H*═C*H*), 2.73−2.62 (m, 8H, PCH_2), 2.35−2.32 (m, 4H, PCH_2CHH'), 2.04 (m, 12H, PCH_2CHH', CH_2CH═CH), 1.42−1.26 (m, 24H, remaining CH_2); ^{31}P{^{1}H} 15.9 (s, $^1J_{PPt}$ = 2594 Hz,[42] 12%), 15.8 (s, $^1J_{PPt}$ = 2585 Hz,[42] 30%), 15.2 (s, $^1J_{PPt}$ = ca. 2579 Hz,[42] 24%), 15.1 ($^1J_{PPt}$ = ca. 2579 Hz,[42] 22%), 15.0 (s, 7%), 14.8 (s, 6%). IR (cm^{-1}, powder film) $\nu_{C\equiv C}$ 2150 (m). MS:[43] 1949 (M^+ (intramolecular metathesis), 100%), no other significant peaks > 1200.

***trans,trans*-(C_6F_5)($Ph_2P(CH_2)_{14}PPh_2$)Pt(C≡C)$_4$Pt($Ph_2P(CH_2)_{14}PPh_2$)-(C_6F_5) (11a).** A Schlenk flask was charged with metathesized **4a** (0.350 g, 0.180 mmol), 10% Pd/C (0.035 g, 0.018 mmol), $ClCH_2CH_2Cl$ (10 mL), and ethanol (20 mL), flushed with H_2, and fitted with a balloon filled with H_2. The mixture was stirred for 7 d. The solvent was removed by rotary evaporation. Then CH_2Cl_2 was added to the residue. The mixture was filtered through an alumina column (7 cm × 1.5 cm), which was rinsed with additional CH_2Cl_2. The solvent was removed from the filtrate by rotary evaporation (0.255 g, 0.130 mmol, 73%). The crude **11a/8a** was purified by preparative thin layer chromatography (silica gel, 60:40 v/v hexanes/CH_2Cl_2). The main (middle) band was extracted to give **11a** as a yellow powder (0.110 g, 0.058 mmol, 32%).[47]

NMR (δ, $CDCl_3$) ^{1}H 7.43−7.17 (m, 40H of 8 Ph), 2.68 (m, 8H, PCH_2), 2.12 (m, 8H, PCH_2CH_2), 1.57 (m, 8H, $PCH_2CH_2CH_2$), 1.50−1.26 (m, 32H, remaining CH_2); ^{13}C{^{1}H}[40,41] 145.7 (dm, $^1J_{CF}$ = 220 Hz, *o* to Pt), 136.2 (dm, $^1J_{CF}$ = 240 Hz, *m*/*p* to Pt), 132.8 (virtual t, $^2J_{CP}$ = 5.7 Hz, *o* to P), 131.9 (virtual t, $^1J_{CP}$ = 27.6 Hz, *i* to P), 130.1 (s, *p* to P), 127.8 (virtual t, $^3J_{CP}$ = 5.0 Hz, *m* to P), 98.5 (s, PtC≡), 94.2 (s, PtC≡*C*), 63.4 (s, PtC≡C*C*), 57.8 (s, PtC≡CC≡*C*), 30.6 (virtual t, $^3J_{CP}$ = 7.8 Hz, $PCH_2CH_2CH_2$), 30.0 (s, CH_2), 29.6 (s, CH_2), 29.3 (s, CH_2), 28.1 (virtual t, $^1J_{CP}$ = 18.5 Hz, PCH_2), 28.0 (s, CH_2), 25.6 (s, PCH_2CH_2); ^{31}P{^{1}H} 15.0 (s, $^1J_{PPt}$ = 2582 Hz).[42]

Alkene Metathesis of 4b. Grubbs' catalyst (0.008 g, 0.01 mmol), **4b** (0.351 g, 0.170 mmol), and CH_2Cl_2 (190 mL) were combined in a procedure analogous to that for **4a**. A similar workup (3 cm × 2 cm alumina column) gave a mixture of cyclized products as a yellow oil (0.327 g, 0.162 mmol, 96%).

NMR (δ, $CDCl_3$) ^{1}H 7.45−7.43 (m, 16H of 8 Ph), 7.34−7.30 (m, 8H of 8 Ph), 7.25−7.22 (m, 16H of 8 Ph), 5.42−5.32 (m, 4H, C*H*═C*H*), 2.70−2.62 (m, 8H, PCH_2), 2.03−1.99 (m, 16H, PCH_2CH_2, CH_2CH═), 1.51−1.29 (m, 40H, remaining CH_2); ^{31}P{^{1}H} 14.5 (s), 14.4 (major, s, $^1J_{PPt}$ = 2571 Hz),[42] 14.3 (s), 14.2 (s). MS:[43] 2005 (M^+ (intramolecular metathesis), 100%), 1837 ([M − C_6F_5]$^+$, 20%).

***trans,trans*-(C_6F_5)($Ph_2P(CH_2)_{16}PPh_2$)Pt(C≡C)$_4$Pt($Ph_2P(CH_2)_{16}PPh_2$)-(C_6F_5) (11b).** A Schlenk flask was charged with metathesized **4b** (0.327 g, 0.162 mmol), 10% Pd/C (0.018 g, 0.017 mmol), $ClCH_2CH_2Cl$ (15 mL), and ethanol (15 mL), flushed with H_2, and fitted with a balloon filled with H_2. The mixture was stirred for 14 d. The solvent was removed by oil pump vacuum. The residue was extracted with CH_2Cl_2. The extract was filtered through an alumina column (2 cm × 2 cm), which was rinsed with CH_2Cl_2 until UV monitoring showed no absorbing material (ca. 40 mL). The solvent was removed from the filtrate by oil pump vacuum to give crude **11b/8b**, which was chromatographed on a silica gel column (30 cm × 1.5 cm, 80:20 v/v hexanes/CH_2Cl_2). The solvent was removed from the first product-containing fraction by oil pump vacuum to give **11b** as a yellow solid (0.165 g, 0.0778 mmol, 48%), dec pt. >200 °C (gradual darkening without melting). Calcd for $C_{100}H_{104}F_{10}P_4Pt_2$: C, 59.76; H, 5.22. Found: C, 58.56; H, 5.22. DSC:[46] exotherm with T_i, 215.7 °C; T_e, 249.6 °C; T_c, 253.5 °C; T_f, 269.5 °C. TGA: weight loss 32%, 276−414 °C.

NMR (δ, $CDCl_3$) ^{1}H 7.45−7.42 (m, 16H of 8 Ph), 7.31−7.27 (m, 8H of 8 Ph), 7.23−7.19 (m, 16H of 8 Ph), 2.72−2.71 (m, 8H, PCH_2), 2.07−2.06 (m, 8H, PCH_2CH_2), 1.57−1.52 (m, 8H $PCH_2CH_2CH_2$), 1.42−1.29 (m, 40H, remaining CH_2); ^{13}C{^{1}H}[40,41] 145.6 (dm, $^1J_{CF}$ = 221 Hz, *o* to Pt), 136.3 (dm, $^1J_{CF}$ = 250 Hz, *m*/*p* to Pt), 132.8 (virtual t, $^2J_{CP}$ = 5.7 Hz, *o* to P), 131.6 (virtual t, $^1J_{CP}$ = 27.8 Hz, *i* to P), 130.2 (s, *p* to P), 127.8 (virtual t, $^3J_{CP}$ = 5.0 Hz, *m* to P), 99.3 (s, PtC≡), 94.0 (s, PtC≡*C*), 63.7 (s, PtC≡C*C*), 57.8 (s, PtC≡CC≡*C*), 30.9 (virtual t, $^3J_{CP}$ = 7.7 Hz, $PCH_2CH_2CH_2$), 29.3 (s, CH_2), 29.0 (s, CH_2), 28.9 (s, CH_2), 28.7 (s, CH_2), 28.5 (s, CH_2), 28.2 (virtual t, $^1J_{CP}$ = 18.2 Hz, PCH_2), 25.9 (s, PCH_2CH_2); ^{31}P{^{1}H} 14.7 (s, $^1J_{PPt}$ = 2575 Hz).[42]

IR (cm^{-1}, powder film) $\nu_{C\equiv C}$ 2142 (m), 2001 (w). UV−vis:[45] 263 (84 000), 290 (105 000), 318 (130 000), 352 (6400), 379 (5500), 410 (2900). MS:[43] 2009 (**11b**$^+$, 100%).

Alkene Metathesis of 4c. Grubbs' catalyst (0.007 g, 0.008 mmol), **4c** (0.277 g, 0.131 mmol), and CH_2Cl_2 (220 mL) were combined in a procedure analogous to that for **4b**. An identical workup gave a mixture of cyclized products as a yellow oil (0.262 g, 0.127 mmol, 97%).

NMR (δ, $CDCl_3$) ^{1}H 7.46−7.40 (m, 16H of 8 Ph), 7.31−7.27 (m, 8H of 8 Ph), 7.24−7.21 (m, 16H of 8 Ph), 5.41−5.28 (m, 4H, C*H*═C*H*), 2.69−2.64 (m, 8H, PCH_2), 2.09−1.98 (m, 16H, PCH_2CH_2, CH_2CH═), 1.50−1.18 (m, 40H, remaining CH_2); ^{31}P{^{1}H} 15.1 (s, $^1J_{PPt}$ = 2583 Hz),[42] 14.6 (s, major, $^1J_{PPt}$ = 2583 Hz),[42] 14.4 (s), 14.2 (s).

***trans,trans*-(C_6F_5)($Ph_2P(CH_2)_{18}PPh_2$)Pt(C≡C)$_4$Pt($Ph_2P(CH_2)_{18}PPh_2$)-(C_6F_5) (11c).** Metathesized **4c** (0.262 g, 0.127 mmol), 10% Pd/C (0.014 g, 0.013 mmol), $ClCH_2CH_2Cl$ (10 mL), ethanol (8 mL), and H_2 were combined in a procedure analogous to that for **11b**. A similar workup gave (from fractions of the silica gel column) **11c** (0.0380 g, 0.0183 mmol, 15%), an **11c/8c** mixture (0.0362 g, 0.175 mmol, 14%; 2:1 by ^{31}P NMR), and **8c** (0.0258 g, 0.0125 mmol, 10%) as yellow powders. Data for **11c**:[48] dec pt. > 200 °C (gradual darkening without melting).

NMR (δ, $CDCl_3$) ^{1}H 7.42−7.38 (m, 16H of 8 Ph), 7.29−7.26 (m, 8H of 8 Ph), 7.22−6.99 (m, 16H of 8 Ph), 2.68−2.65 (m, 8H, PCH_2), 1.96−1.95 (m, 8H, PCH_2CH_2), 1.54−1.49 (m, 8H, $PCH_2CH_2CH_2$), 1.35−1.27 (m, 56H, remaining CH_2); ^{13}C{^{1}H}[40,41] 146.2 (dm, $^1J_{CF}$ = 245 Hz, *o* to Pt), 136.8 (dm, $^1J_{CF}$ = 247 Hz, *m*/*p* to Pt), 133.2 (virtual t, $^2J_{CP}$ = 5.7 Hz, *o* to P), 131.9 (virtual t, $^1J_{CP}$ = 27.8 Hz, *i* to P), 130.7 (s, *p* to P), 128.2 (virtual t, $^3J_{CP}$ = 5.0 Hz, *m* to P), 101.0 (s, PtC≡), 94.0 (s, PtC≡*C*), 63.8 (s, PtC≡C*C*), 58.1 (s, PtC≡CC≡*C*, 31.7 (virtual t, $^3J_{CP}$ = 7.5 Hz, $PCH_2CH_2CH_2$), 29.5 (s, triple intensity, 3 CH_2), 29.4 (s, CH_2), 29.3 (s, CH_2), 29.1 (s, CH_2), 28.5 (virtual t, $^1J_{CP}$ = 17.9 Hz, PCH_2), 26.6 (s, PCH_2CH_2); ^{31}P{^{1}H} 14.5 (s, $^1J_{PPt}$ = 2570 Hz).[42]

IR (cm^{-1}, powder film) $\nu_{C\equiv C}$ 2146 (m), 2001 (w). UV−vis:[45] 263 (88 000), 290 (112 000), 319 (138 000), 352 (6300), 379 (5400), 410 (2900). MS:[43] 2066 (**11c**$^+$, 100%).

Alkene Metathesis of 4d. Grubbs' catalyst (ca. half of 0.009 g, 0.01 mmol), **4d** (0.327 g, 0.150 mmol), and CH_2Cl_2 (250 mL) were combined in a procedure analogous to that for **4b**. An identical workup gave a mixture of cyclized products as a yellow oil (0.305 g, 0.144 mmol, 96%).

NMR (δ, $CDCl_3$) ^{1}H 7.45−7.43 (m, 16H of 8 Ph), 7.33−7.30 (m, 8H of 8 Ph), 7.26−7.22 (m, 16H of 8 Ph), 5.43−5.30 (m, 4H, C*H*═C*H*), 2.70−2.63 (m, 8H, PCH_2), 2.03−1.99 (m, 16H, PCH_2CH_2, CH_2CH═), 1.51−1.29 (m, 48H, remaining CH_2); ^{31}P{^{1}H} 14.5 (s, major, $^1J_{PPt}$ = 2567 Hz),[42] 14.4 (s), 14.2 (s). MS:[43] 2118 (M^+ (intramolecular metathesis), 100%).

***trans,trans*-(C_6F_5)($Ph_2P(CH_2)_{20}PPh_2$)Pt(C≡C)$_4$Pt($Ph_2P(CH_2)_{20}PPh_2$)-(C_6F_5) (11d).** Metathesized **4d** (0.305 g, 0.144 mmol), 10% Pd/C (0.015 g, 0.014 mmol), $ClCH_2CH_2Cl$ (8 mL), ethanol (5 mL), and H_2 were combined in a procedure analogous to that for **11c**. An identical workup gave **11d** (0.0551 g, 0.0259 mmol, 18%), an **11d**/**8d** mixture (0.0982

(47) A complementary sequence is given in the Supporting Information.

(48) A satisfactory microanalysis was not obtained for this compound.

g, 0.0463 mmol, 32%; 2:1 by ^{31}P NMR), and **8d** (0.0488 g, 0.0230 mmol, 16%) as yellow powders. Data for **11d**: dec pt. >190 °C (gradual darkening without melting). Calcd for $C_{108}H_{120}F_{10}P_4Pt_2$: C, 61.12; H, 5.70. Found: C, 60.82; H, 5.71. DSC:[46] exotherm with T_i, 102.1 °C; T_e, 113.2 °C; T_p, 121.7 °C; T_c, 126.6 °C; T_f, 137.7 °C; endotherm with T_i, 197.7 °C; T_e, 218.7 °C; T_p, 225.2 °C; T_c, 226.9 °C; T_f, 230.5 °C. TGA: weight loss 29%, 272−402 °C.

NMR (δ, $CDCl_3$) ^{1}H 7.42−7.38 (m, 16H of 8 Ph), 7.30−7.26 (m, 8H of 8 Ph), 7.24−7.19 (m, 16H of 8 Ph), 2.63−2.62 (m, 8H, PCH_2), 1.92 (m, 8H, PCH_2CH_2), 1.52 (m, 8H, $PCH_2CH_2CH_2$), 1.23−1.13 (m, 60H, remaining CH_2); ^{13}C{^{1}H}[40,41] 132.7 (virtual t, $^2J_{CP}$ = 5.8 Hz, *o* to P), 131.3 (virtual t, $^1J_{CP}$ = 27.9 Hz, *i* to P), 130.1 (s, *p* to P), 127.7 (virtual t, $^3J_{CP}$ = 5.0 Hz, *m* to P), 93.4 (s, PtC≡*C*), 68.2 (s, PtC≡*C*C), 57.5 (s, PtC≡CC≡*C*), 31.1 (virtual t, $^3J_{CP}$ = 7.7 Hz, $PCH_2CH_2CH_2$), 29.0 (s, CH_2), 28.94 (s, CH_2), 28.93 (s, CH_2), 28.87 (s, CH_2), 28.7 (s, CH_2), 28.6 (s, CH_2), 27.9 (virtual t, $^1J_{CP}$ = 18.1 Hz, PCH_2), 25.5 (s, PCH_2CH_2); ^{31}P{^{1}H} 14.6 (s, $^1J_{PPt}$ = 2569 Hz).[42]

IR (cm^{-1}, powder film) $\nu_{C\equiv C}$ 2144 (m), 2001 (w). UV−vis:[45] 263 (87 500), 290 (111 000), 318 (136 000), 352 (6400), 379 (5500), 410 (3000). MS:[43] 2121 (**11d**$^+$, 100%), 1953 ([**11d** − C_6F_5]$^+$, 10%).

***trans*-(C_6F_5)($Ph_2P(CH_2)_8CH{=}CH_2$)$_2$Pt(C≡C)$_3$SiEt$_3$ (12c).** A three-necked flask was charged with **3c** (0.640 g, 0.604 mmol), acetone (20 mL), and HC≡CSiEt$_3$ (1.20 mL, 12.7 mmol) and fitted with a gas inlet needle and a condenser chilled via circulating −18 °C ethanol.[44] A Schlenk flask was charged with CuCl (0.200 g, 2.02 mmol) and acetone (30 mL), and TMEDA (0.400 mL, 2.40 mmol) was added with stirring. After 0.5 h, stirring was halted (blue supernatant/yellow-green solid). Then O_2 was bubbled through the three-necked flask with stirring, and the solution was heated to 65 °C. The blue supernatant was added in portions over 2 h. After an additional 0.5 h, the solvent was removed by rotary evaporation and oil pump vacuum. The residue was extracted with hexanes (2 × 5 mL) and then toluene (3 × 5 mL). The extracts were passed in sequence through an alumina column (6 cm × 2 cm), which was rinsed with toluene. The solvent was removed from the toluene fractions by rotary evaporation. The residue was chromatographed on a silica gel column (20 cm × 2.5 cm, 90:10 v/v hexanes/CH_2Cl_2). The solvent was removed from the product-containing fractions by oil pump vacuum to give **12c** as a yellow oil (0.525 g, 0.438 mmol, 73%). Elution with 70:30 v/v hexanes/CH_2Cl_2 gave **4c** (0.122 g, 0.058 mmol, 19%). Data for **12c**: Calcd for $C_{62}H_{73}F_5P_2PtSi$: C, 62.14; H, 6.32. Found: C, 61.83; H, 6.32.

NMR (δ, $CDCl_3$): ^{1}H 7.52−7.47 (m, 8H of 4 Ph), 7.37−7.33 (m, 4H of 4 Ph), 7.30−7.26 (m, 8H of 4 Ph), 5.83 (ddt, 2H, $^3J_{HHtrans}$ = 17.0 Hz, $^3J_{HHcis}$ = 10.2 Hz, $^3J_{HH}$ = 6.7 Hz, CH═), 5.02 (br d, 2H, $^3J_{HHtrans}$ = 17.0 Hz, ═CH$_E$*H*$_Z$), 4.95 (br d, 2H, $^3J_{HHcis}$ = 10.2 Hz, ═C*H*$_E$H$_Z$), 2.61−2.58 (m, 4H, PCH_2), 2.09−2.04 (m, 4H, C*H*$_2$CH═), 1.84−1.82 (m, 4H, PCH_2CH_2), 1.43−1.32 (m, 20H, remaining CH_2), 0.97 (t, 9H, $^3J_{HH}$ = 7.9 Hz, CH_3), 0.57 (q, 6H, $^3J_{HH}$ = 7.9 Hz, $SiCH_2$); ^{13}C{^{1}H}[40,41] 145.9 (dm, $^1J_{CF}$ = 237 Hz, *o* to Pt), 139.1 (s, CH═), 136.6 (dm, $^1J_{CF}$ = 235 Hz, *m*/*p* to Pt), 132.9 (virtual t, $^2J_{CP}$ = 5.8 Hz, *o* to P), 131.2 (virtual t, $^1J_{CP}$ = 28.0 Hz, *i* to P), 130.4 (s, *p* to P), 127.9 (virtual t, $^3J_{CP}$ = 5.1 Hz, *m* to P), 114.1 (s, ═CH_2), 102.7 (s, PtC≡), 93.1 (s, PtC≡*C*), 91.0 (s, *C*≡CSi), 80.6 (s, ≡CSi), 65.7 (s, PtC≡C*C*), 55.9 (s, PtC≡CC≡*C*), 33.8 (s, *C*H$_2$CH═), 31.2 (virtual t, $^3J_{CP}$ = 7.6 Hz, $PCH_2CH_2CH_2$), 29.3 (s, CH_2), 29.0 (s, double intensity, 2 CH_2), 28.9 (s, CH_2), 28.2 (virtual t, $^1J_{CP}$ = 18.1 Hz, PCH_2), 25.5 (s, PCH_2CH_2), 7.3 (s, CH_3), 4.3 (s, $SiCH_2$); ^{31}P{^{1}H} 14.2 (s, $^1J_{PPt}$ = 2558 Hz).[42]

IR (cm^{-1}, oil film) $\nu_{C\equiv C}$ 2150 (m), 2018 (m). MS:[43] 1198 (**12c**$^+$, 40%), 1011 ([**12c** − C_6SiEt_3]$^+$, 100%), 842 ([**12c** − C_6SiEt_3 − C_6F_5]$^+$, 40%).

***trans*,*trans*-(C_6F_5)($Ph_2P(CH_2)_8CH{=}CH_2$)$_2$Pt(C≡C)$_6$Pt($Ph_2P(CH_2)_8CH{=}CH_2$)$_2$(C_6F_5) (13c).** Complex **12c** (0.287 g, 0.244 mmol), acetone (15 mL), CuCl (0.260 g, 2.63 mmol), acetone (15 mL), TMEDA (0.520 mL, 3.12 mmol), *n*-Bu_4N^+ F^- (0.050 mL, 0.050, 1 M in THF/5 wt % H_2O), Me_3SiCl (0.040 mL, 0.32 mmol), and O_2 were combined in a procedure analogous to that for **8b**. A similar workup (3 cm × 2 cm alumina column; 20 cm × 2 cm silica gel column, 90:10 v/v hexanes/CH_2Cl_2) gave **13c** as a yellow oil that solidified over the course of several days (0.170 g, 0.0785 mmol, 64%). Calcd for $C_{112}H_{116}F_{10}P_4Pt_2$: C, 62.10; H, 5.40. Found: C, 61.31; H, 5.65. DSC:[46] endotherm with T_i, 100.3 °C; T_e, 123.2 °C; T_p, 124.9 °C; T_c, 126.9 °C; T_f, 149.8 °C. TGA: weight loss 38%, 225−414 °C.

NMR (δ, $CDCl_3$) ^{1}H 7.47−7.43 (m, 16H of 8 Ph), 7.36−7.32 (m, 8H of 8 Ph), 7.28−7.24 (m, 16H of 8 Ph), 5.80 (ddt, 4H, $^3J_{HHtrans}$ = 17.0 Hz, $^3J_{HHcis}$ = 10.2 Hz, $^3J_{HH}$ = 6.7 Hz, CH═), 4.98 (br d, 4H, $^3J_{HHtrans}$ = 17.1 Hz, ═CH$_E$*H*$_Z$), 4.91 (br d, 4H, $^3J_{HHcis}$ = 10.2 Hz, ═C*H*$_E$H$_Z$), 2.55−2.51 (m, 8H, PCH_2), 2.05−1.99 (m, 8H, C*H*$_2$CH═), 1.75−1.73 (m, 8H, PCH_2CH_2), 1.36−1.26 (m, 40H, remaining CH_2); ^{13}C{^{1}H}[40,41] 139.2 (s, CH═), 136.6 (dm, $^1J_{CF}$ = 251 Hz, *m*/*p* to Pt), 132.9 (virtual t, $^2J_{CP}$ = 5.7 Hz, *o* to P), 131.0 (virtual t, $^1J_{CP}$ = 28.0 Hz, *i* to P), 130.4 (s, *p* to P), 128.0 (virtual t, $^3J_{CP}$ = 5.1 Hz, *m* to P), 114.1 (s, ═CH_2), 105.4 (s, PtC≡), 93.4 (s, PtC≡*C*), 65.5, 63.0, 61.0, 57.1 (4 s, PtC≡C*C*≡*CC*≡*C*), 33.8 (s, *C*H$_2$CH═), 31.2 (virtual t, $^3J_{CP}$ = 7.5 Hz, $PCH_2CH_2CH_2$), 29.2 (s, CH_2), 29.09 (s, CH_2), 29.06 (s, CH_2), 28.9 (s, CH_2), 28.2 (virtual t, $^1J_{CP}$ = 17.5 Hz, PCH_2), 25.4 (s, PCH_2CH_2); ^{31}P{^{1}H} 13.9 (s, $^1J_{PPt}$ = 2544 Hz).[42]

IR (cm^{-1}, oil film) $\nu_{C\equiv C}$ 2132 (m), 2094 (m), 1997 (w). UV−vis (1.25 × 10^{-6} M):[45] 311 (75 500), 332 (201 000), 354 (315 000). MS:[43] 2166 (**13c**$^+$, 20%), 1010 ([(C_6F_5)Pt($Ph_2P(CH_2)_8CH{=}CH_2$)$_2$]$^+$, 100%).

Alkene Metathesis of 13c. A two-necked flask was charged with Grubbs' catalyst (ca. half of 0.014 g, 0.017 mmol) and CH_2Cl_2 (300 mL) and fitted with a condenser and a dropping funnel. The solution was refluxed. The dropping funnel was charged with a solution of **13c** (0.548 g, 0.251 mmol) in CH_2Cl_2 (50 mL). One-half of the solution was added over 0.5 h. After 2 h, the remaining catalyst was added, followed by the remaining **13c**. After an additional 2 h, the solvent was removed by oil pump vacuum, and CH_2Cl_2 (2 × 3 mL) was added. The sample was transferred in two portions to an alumina column (3 cm × 2.5 cm), which was rinsed with CH_2Cl_2 until UV monitoring showed no absorbing material (ca. 50 mL). The solvent was removed by oil pump vacuum to give a mixture of cyclized products as a yellow oil (0.402 g, 0.187 mmol, 75%).

NMR (δ, $CDCl_3$) ^{31}P{^{1}H} 14.9 (s, $^1J_{PPt}$ = 2564 Hz),[42] 14.4 (s), 14.2 (s, $^1J_{PPt}$ = 2652 Hz),[42] 14.1 (s, major, $^1J_{PPt}$ = 2556 Hz),[42] 13.9 (s). MS:[43] 2110 (*M*$^+$ (intramolecular metathesis), 100%), 982 ([(C_6F_5)Pt($Ph_2P(CH_2)_8CH{=}CH(CH_2)_8PPh_2$)]$^+$, 60%), 815 ([Pt($Ph_2P(CH_2)_8CH{=}CH(CH_2)_8PPh_2$)]$^+$, 50%).

***trans*,*trans*-(C_6F_5)($Ph_2P(CH_2)_{18}PPh_2$)Pt(C≡C)$_6$Pt($Ph_2P(CH_2)_{18}PPh_2$)(C_6F_5) (14c).** Metathesized **13c** (0.402 g, 0.187 mmol), 10% Pd/C (0.026 g, 0.025 mmol), $ClCH_2CH_2Cl$ (15 mL), ethanol (15 mL), and H_2 were combined in a procedure analogous to that for **11b**. An identical workup gave **14c** as a yellow powder (0.080 g, 0.038 mmol, 20%), dec pt. > 230 °C.

NMR (δ, $CDCl_3$) ^{1}H 7.40−7.38 (m, 16H of 8 Ph), 7.30−7.28 (m, 8H of 8 Ph), 7.22−7.20 (m, 16H of 8 Ph), 2.71−2.68 (m, 8H, PCH_2), 2.10−2.06 (m, 8H, PCH_2CH_2), 1.54−1.50 (m, 8H, $PCH_2CH_2CH_2$), 1.40−1.36 (m, 8H, $PCH_2CH_2CH_2CH_2$), 1.25−1.18 (m, 40H, remaining CH_2); ^{13}C{^{1}H}[40,41] 143.8 (dd, $^1J_{CF}$ = 225 Hz, $^2J_{CF}$ = 30 Hz, *o* to Pt), 136.5 (dm, $^1J_{CF}$ = 242 Hz, *m*/*p* to Pt), 132.8 (virtual t, $^2J_{CP}$ = 6.0 Hz, *o* to P), 131.0 (virtual t, $^1J_{CP}$ = 27.9 Hz, *i* to P), 130.4 (s, *p* to P), 127.9 (virtual t, $^3J_{CP}$ = 5.0 Hz, *m* to P), 103.8 (s, PtC≡), 93.6 (s, PtC≡*C*), 65.0, 62.7, 61.0, 57.3 (4 s, PtC≡C*C*≡*CC*≡*C*), 30.9 (virtual t, $^3J_{CP}$ = 7.9 Hz, $PCH_2CH_2CH_2$), 30.2 (s, CH_2), 30.1 (s, CH_2), 30.03 (s, CH_2), 29.97 (s, CH_2), 28.4 (virtual t, $^1J_{CP}$ = 18.2 Hz, PCH_2), 25.7 (s, PCH_2CH_2); ^{31}P{^{1}H} 14.5 (s, $^1J_{PPt}$ = 2554 Hz).[42]

IR (cm^{-1}, powder film) $\nu_{C\equiv C}$ 2131 (m), 2092 (s), 1996 (m); UV−vis (1.25 × 10^{-6} M):[45] 312 (79 200), 331 (234 000), 354 (361 000). MS:[43] 2113 (**14c**$^+$, 100%), 1945 ([**14c** − C_6F_5]$^+$, 8%).

Alkene Metathesis of 13d. Grubbs' catalyst (0.010 g, 0.013 mmol), CH_2Cl_2 (150 mL), **13d** (0.396 g, 0.178 mmol), and CH_2Cl_2 (50 mL) were combined in a procedure analogous to that for **13c**. An identical

workup gave a mixture of cyclized products as a yellow powder (0.292 g, 0.135 mmol, 76%).

NMR (δ, $CDCl_3$) $^{31}P\{^1H\}$ 16.6 (s), 13.9 (s), 13.6 (s), 13.3 (s, major), 13.2 (s), 13.1 (s, major), 11.8 (s), 11.7 (s). MS:[43] 2165 (M^+ (intramolecular metathesis), 100%).

***trans,trans*-(C_6F_5)($Ph_2P(CH_2)_{20}PPh_2$)Pt($C{\equiv}C)_6$Pt($Ph_2P(CH_2)_{20}PPh_2$)-(C_6F_5) (14d).** Metathesized **13d** (0.292 g, 0.135 mmol), 10% Pd/C (0.026 g, 0.025 mmol), $ClCH_2CH_2Cl$ (15 mL), ethanol (15 mL), and H_2 were combined in a procedure analogous to that for **11b**. An identical workup gave **14d** as a yellow powder (0.089 g, 0.032 mmol, 24%), dec pt. > 220 °C. Calcd for $C_{112}H_{120}F_{10}P_4Pt_2$: C, 61.99; H, 5.57. Found: C, 60.77; H, 5.58.

NMR (δ, $CDCl_3$) ^1H 7.42−7.39 (m, 16H of 8 Ph), 7.31−7.28 (m, 8H of 8 Ph), 7.25−7.22 (m, 16H of 8 Ph), 2.73−2.68 (m, 8H, PCH_2), 2.10−2.07 (m, 8H, PCH_2CH_2), 1.54−1.50 (m, 8H, $PCH_2CH_2CH_2$), 1.38−1.35 (m, 8H, $PCH_2CH_2CH_2CH_2$), 1.32−1.24 (m, 68H, remaining CH_2); $^{13}C\{^1H\}$[40,41] 145.6 (dm, $^1J_{CF}$ = 239 Hz, *o* to Pt), 132.8 (dm, $^1J_{CF}$ = 253 Hz, *m*/*p* to Pt), 132.8 (virtual t, $^2J_{CP}$ = 6.0 Hz, *o* to P), 131.5 (virtual t, $^1J_{CP}$ = 27.8 Hz, *i* to P), 130.4 (s, *p* to P), 128.0 (virtual t, $^3J_{CP}$ = 5.1 Hz, *m* to P), 93.6 (s, PtC≡*C*), 62.8, 61.0, 57.1, 53.4 (4 s, PtC≡C*C*≡*CC*≡*C*), 30.9 (virtual t, $^3J_{CP}$ = 7.9 Hz, $PCH_2CH_2CH_2$), 29.9 (s, CH_2), 29.8 (s, CH_2), 29.9−28.6 (several signals, remaining CH_2), 28.4 (virtual t, $^1J_{CP}$ = 18.2 Hz, PCH_2), 25.7 (s, PCH_2CH_2). $^{31}P\{^1H\}$ 14.5 (s, $^1J_{PPt}$ = 2576 Hz).[42]

IR (cm^{-1}, powder film) $\nu_{C\equiv C}$ 2131 (m), 2092 (s), 1996 (m); UV−vis (1.25×10^{-6} M):[45] 312 (67 200), 333 (181 000), 354 (306 000). MS:[43] 2170 (**14d**$^+$, 100%).

Acknowledgment. We thank the Deutsche Forschungsgemeinschaft (SFB 583), the US NSF (CHE-9732605), Johnson Matthey (platinum loan), the Ministerio de Educación y Ciencia, and the Fulbright Commission (Fellowships, J.M.M.-A.) for support, Dr. Qinglin Zheng for the sample of $Me_3Sn(C{\equiv}C)_2SiMe_3$, and Ms. Helene Kuhn for technical assistance.

Supporting Information Available: Continuation of the Experimental Section, including general methods, syntheses and characterization of higher homologues,[38] figures of NMR spectra and cyclic voltammetry traces, details of crystallographic data collection and refinement,[49] and tables of spectroscopic and crystallographic data. This material is available free of charge via the Internet at http://pubs.acs.org.

JA071612N

(49) Additional data are available from the Cambridge Crystallographic data Centre via the following CCDC numbers: 624437 (**7b**), 624434 (**8a**·EtOH), 624436 (**8c**·C_6H_{12}), 295840 (**8d**), 295839 (**11d**), 624435 (**14d**).